UNITED NATIONS EDUCATIONAL, SCIENTIFIC AND CULTURAL ORGANIZATION
INTERNATIONAL ATOMIC ENERGY AGENCY
INTERNATIONAL CENTRE FOR THEORETICAL PHYSICS
I.C.T.P., P.O. BOX 586, 34100 TRIESTE, ITALY, CABLE: CENTRATOM TRIESTE

SMR/930 - 7

"Workshop on El Niño, Southern Oscillation and Monsoon"
15 - 26 July 1996

"South Asian Monsoon & the Tropospheric Biennial Oscillation (TBO)"

G. MEEHL
NCAR
Boulder, CO
USA

---

submitted to J. Climate

THE SOUTH ASIAN MONSOON AND THE TROPOSPHERIC BIENNIAL OSCILLATION (TBO)

Gerald A. Meehl

National Center for Atmospheric Research
Boulder, CO 80307
meehl@ncar.ucar.edu

20 June 1996

Abstract.

A mechanism is described that involves the south Asian monsoon as an active part of the tropospheric biennial oscillation (TBO) described in previous studies. This mechanism depends on coupled interactions between land-atmosphere-ocean in the Indian sector, large-scale atmospheric east-west circulations in the tropics, convective heating anomalies over Africa and the Pacific, and tropical-midlatitude interactions in the Northern Hemisphere. A key element for the monsoon role in the TBO is land-sea or meridional tropospheric temperature contrast, with area-averaged surface temperature anomalies over south Asia that are able to persist on a one year time scale without the heat storage characteristics that contribute to this memory mechanism in the ocean. Results from a global coupled general circulation model show that soil moisture anomalies contribute to land surface temperature anomalies (through latent heat flux anomalies) for only one season after the summer monsoon. A global atmospheric GCM in perpetual January mode is run with observed SSTs with specified convective heating anomalies to demonstrate that convective heating anomalies elsewhere in the tropics associated with the coupled ocean-atmosphere biennial mechanism can contribute to altering seasonal mid-latitude circulation. These changes in the midlatitude longwave pattern, forced by a combination of tropical convective heating anomalies over east Africa, southeast Asia, and the western Pacific (in association with SST anomalies), is then able to maintain temperature anomalies over south Asia via advection through winter and spring to set up the land-sea meridional tropospheric temperature contrast for the subsequent monsoon. The role of the Indian Ocean, then, is to provide a moisture source and a low amplitude coupled response component for meridional temperature contrast to help drive the south Asian monsoon. The role of the Pacific is to produce shifts in regionally coupled convection-SST anomalies. These regions are tied together and mutually interact

via the large-scale east-west circulation in the atmosphere and contribute to altering midlatitude circulations as well. The coupled model results and experiments with an atmospheric GCM that includes specified convective heating anomalies suggest that the influence of south Asian snow cover in the monsoon is not a driving force by itself, but is symptomatic of the larger-scale shift in the midlatitude longwave pattern associated with tropical SST and convective heating anomalies.

1. Introduction

Coupled interactions between ocean and atmosphere have previously been identified (Meehl, 1987,1993,1994a) as contributing to a mechanism that produces a biennial component of interannual variability in the troposphere in the tropical Indian and Pacific regions (the tropical or tropospheric biennial oscillation or TBO). Biennial signals in various parts of those areas have been noted by a number of studies (e.g. Trenberth, 1975; Nicholls, 1978, 1979, 1984, Tomita and Yasunari, 1996; Clarke et al., 1996). The role of air sea coupling (e.g. Brier, 1978) has been central to all studies of such biennial oscillations, and several of those studies have linked the biennial component of variability to the Southern Oscillation. In particular, Meehl (1987) noted this linkage involved the seasonal cycle and postulated that peaks in the biennial cycle were manifested via a similar set of processes as the tropical Pacific warm and cold extremes in the Southern Oscillation. Subsequent studies have confirmed these earlier results (e.g. Terray, 1995; Shen and Lau, 1996; Tomita and Yasunari, 1996), and have also further quantified the biennial component of tropospheric variability in the tropical Pacific and/or Indian regions in SST and surface wind (Lau and Sheu, 1988; Rasmusson et al., 1990; Barnett, 1991; Kutsuwada, 1991; Ropelewski et al., 1992; Jiang et al., 1995; Clarke et al., 1996). Biennial tendencies have also been noted to involve ocean dynamics in the western Pacific (e.g. Lukas, 1988; Masumoto and Yamagata, 1991). The active role of the east Asian summer monsoon in the TBO has been emphasized by Lau (1992) and Shen and Lau (1995) as well as associated coupled air-sea interaction in the South China Sea/maritime continent region (Tomita and Yasunari, 1996; Ju and Slingo, 1995; Soman and Slingo, 1996: Clarke et al., 1996; Clarke et al., 1996).

It has been suggested that the TBO may arise from interaction between the annual cycle and the El Nino/Southern Oscillation (ENSO) cycle (Goswami, 1995). However, that study assumed that the ENSO cycle is a fixed mode of the climate system

with a set period of 4 years. However, if the TBO and ENSO operate with similar mechanisms, the TBO could be a determining factor in setting up the ENSO cycle and monsoon interactions, and not vice versa (Shen and Lau, 1995). More recently, modeling results have suggested that the Indian summer monsoon could generate an internal biennial oscillation without any interactions with other components of the climate system, or possibly through interaction of intraseasonal oscillations with the annual cycle (Goswami and Manabe, 1996). Yet other modeling studies have demonstrated the fundamental role of SST anomalies (and thus the role of interannual atmosphere-ocean interactions) in the Indo-Australian monsoons (Kitoh, 1992; Palmer et al., 1992; Chen and Yen, 1994) and in the TBO (Alexander and Weickmann, 1995). Thus the possibility exists that the south Asian monsoon could generate it's own biennial oscillation independent of other interactions or in concert with irregular ENSO variability (e.g. Jin et al., 1994). But it would appear equally plausible that the timing, strength and nature of the TBO involves multiscale land-atmosphere-ocean interactions such that the south Asian monsoon plays an interactive role in larger-scale tropical interannual variability (Yasunari, 1990) that could provide deterministic links to assist in forecasting monsoon rainfall (Lau and Yang, 1996).

Meehl (1987) used Indian monsoon rainfall as an index of coupled air-sea interactions over the entire Indian and Pacific regions that produce a tropospheric biennial signal in about two thirds of the years considered. It was also noted that SST anomalies in the tropical Indian and Pacific Oceans varied in phase in the biennial and Southern oscillations, and that Indian monsoon rainfall was inherently tied to the TBO. There have been attempts to link the stratospheric quasi-biennial oscillation (QBO) to interannual variability in the troposphere involved with the Southern Oscillation (e.g. Gray et al, 1992). However, the work cited above dealing with with the TBO has not yet been linked to the QBO a priori. Such linkages may indeed exist but are beyond the scope of

the present paper.

Since the TBO is postulated to be manifested as extremes in the Southern Oscillation (SO) and the Indian monsoon has been shown to be closely linked to the SO via the large-scale east-west circulation in the atmosphere (e.g. Webster and Yang, 1992; Ju and Slingo, 1995), it is clear that the Indian monsoon is closely connected with the TBO. However, since air-sea interaction is postulated as the central mechanism for the TBO in those regions, it is unclear exactly what role the Indian monsoon plays either directly or indirectly in the TBO. The purpose of this paper is to specifically address the role of the Indian monsoon (or more generally the south Asian summer monsoon) in the TBO. This paper will also address the role of tropical-midlatitude interactions in greater detail since the TBO and monsoon interactions most likely involve large time and space scale interactions (Webster and Yang, 1992; Meehl, 1987, 1994a; Tomita and Yasunari, 1996; Nigam, 1994; Yang et al., 1996; Yasunari and Seki, 1992; Chen and Yen, 1993,1994).

2. The Coupled Ocean-atmosphere Biennial Mechanism

As first described by Meehl (1987) and later elaborated on by Meehl (1993), the biennial mechanism involving air-sea coupling can be described at a given location schematically by the diagram in Fig. 1a. For this mechanism to work, there are several premises that must be satisfied. First, the seasonal cycle must play a role such that convection is locally strong during one season per year. Second, the air-sea coupling must be strong only during that one season when the convection is locally strong. Third, upper ocean heat content and SSTs must be affected during that season via vigorous air-sea coupling such that anomalies set up during that season persist for one year. Meehl (1987, his Figure 3a) shows a Hovmuller diagram of the long term mean seasonal cycle of outgoing longwave radiation (OLR) averaged from 30N to 30S. Convection is locally strong

once per year at all locations in the Indian-Pacific region as the convective maximum translates from west to east and north to south going from northern summer to southern summer (Meehl, 1987; Murakami and Wang, 1993), even in areas where the ITCZ passes overhead twice per year. This demonstrates that east-west atmospheric circulations are a dominant factor in the seasonal cycle as well as in their more familiar role in interannual variability.

To summarize the biennial mechanism involving air-sea coupling (Fig. 1a), if the SST at a given location starts out relatively warm (as in the right panel), convective activity associated with the seasonal cycle encounters this relatively warm water at the time of year of the local convective maximum (or local "rainy season"). The relatively warm water enhances the convection with increased evaporation and moisture convergence (top panel). This produces relatively strong winds, high latent heat flux, and enhanced mixing that acts to cool the upper ocean. At the end of that season, the convective maximum moves on with the seasonal cycle leaving the upper ocean relatively cool. Via alterations of upper ocean heat content (Meehl, 1993) the ocean provides the memory to retain the relatively cool conditions (left panel in Fig. 1a) until a year later when the convective maximum associated with the seasonal cycle again arrives at that location (bottom panel of Fig. 1a). The cool SSTs, associated decreases of evaporation and reduced low-level moisture convergence, all contribute to weaker convective activity. Accordingly, the low level winds are weaker and there is proportionately less latent heat flux. Consequently the SSTs are left relatively warm at the end of that season in conjunction with higher heat content in the upper ocean (Meehl, 1993). This provides the memory for the relatively warm SSTs to persist (right panel in Fig. 1a) until a year later when the convective maximum is again relatively strong, and so on.

In this conceptual view, the coupled system exists in two states relative to each other--one warm and one cool. In the idealized case, the average (or zero) state never

occurs. The mean climate is simply the arithmetic average of the relatively warm and cool states. However, as shown by Rasmusson et al. (1990) and Ropelewski et al. (1992) what actually seems to happen is that the TBO is superimposed on a low-frequency component of variability such that the interactions between the biennial and low frequency components could be manifested as extremes in the SO. Yet the conceptual model of Fig. 1a is useful to visualize the coupled processes that could occur to actually produce the TBO. In this view dynamical coupling between ocean and atmosphere in conjunction with the seasonal cycle of convection over the tropical Indian and Pacific regions and the large-scale east-west circulation in the atmosphere combine to produce the TBO. This precludes the TBO simply occurring as incidental interaction between the annual cycle and the ENSO cycle. However, the interaction of the TBO with the seasonal cycle could be intermittent (Barnett, 1991), and the amplitude in any given year could vary (Terray, 1995). This could partly explain why the TBO does not have higher total amplitude in the studies of Rasmusson et al. (1990) and Ropelewski et al. (1992).

Since Meehl (1987) and others have shown that the south Asian monsoon has links to the TBO, it is possible to pose a set of processes that could make the monsoon an active participant in working with large-scale atmospheric circulations and air-sea interaction mechanisms to produce the TBO. For this to happen, there should be (at least) coupled land-ocean-atmosphere interactions that directly involve the seasonal cycle as was noted for the air-sea mechanism described above. Fig. 1b shows a schematic of possible processes that could actively involve the south Asian monsoon in the TBO. Here, there are similar premises to those posed for the air-sea mechanism. First, convection must be strong during only one season per year. This premise is easy to satisfy since the south Asian monsoon has a well known once-per-year precipitation maximum during northern summer. Second, land-atmosphere coupling must be strong during that season. Third, there must be a set of processes that provide a one year timescale mem

ory for land surface temperature anomalies. This function was performed by heat storage in the ocean for the air-sea mechanism. This last premise is more difficult to satisfy for land since there is much less capability for heat storage. This issue will be addressed in more detail later.

In addition to the fundamental difference of surface type between land and ocean, the atmosphere-land biennial mechanism must work somewhat differently than the atmosphere-ocean mechanism. The latter relies mainly on local air-sea interaction (along with low-level moisture convergence and large scale linkages associated with the atmospheric east-west circulation) for most of the coupled processes that contribute to either a strong or weak convective maximum. For the south Asian monsoon, the fundamental concept that is important for producing a biennial signal is land-sea temperature contrast or, more accurately, north-south meridional tropospheric temperature gradient. This is the basic forcing of the monsoon (e.g. Webster, 1987) such that enhanced meridional temperature contrast is associated, in the observations, with strong Asian summer monsoons and vice versa for weak monsoons (e.g. Li and Yanai, 1996). This basic phenomenon also appears as a fundamental element of model simulations of the monsoon as well with stronger land-sea or meridional tropospheric temperature contrast at the beginning of the monsoon season in associated with greater the monsoon precipitation over south Asia in a variety of GCMs with the same fixed SSTs (Meehl, 1994b).

The role of land-sea or meridional tropospheric temperature contrast in tropical rainfall regimes has been well-studied. For example, Charney et al. (1977) showed that increased land albedo produced cooler land temperatures, reduced land-sea temperature contrast, and reduced precipitation over land in the West African monsoon. A recent GCM study has demonstrated this relationship that includes the associated increase in soil moisture with reduced tropical land albedo and increased precipitation (Lofgren, 1995). Other GCM studies of paleoclimate have shown that changes in solar parameters can enhance summer heating of south Asia, increase land-sea temperature contrast, and produce a stronger south Asian monsoon (e.g. Kutzbach et al., 1993). The role of snow cover in altering surface temperature and land-sea temperature contrast was first put forth by Blanford (1884), and was shown for more recent observations by Hahn and Shukla (1976). These studies (and others, see Shukla, 1987) noted a tendency for enhanced winter and spring snow cover over south Asia to be followed by below normal monsoon rainfall. The mechanism involves proportionately more solar radiation being reflected by the excessive snow cover, and a subsequent wetter land surface as the excessive snow cover melts. Both these processes act to produce colder land temperatures, reduced land-sea temperature contrast, weakened meridional tropospheric temperature gradient, and a weaker monsoon. These mechanisms have been studied more recently and shown to work in GCM studies (e.g. Barnett et al., 1989; Yasunari et al., 1991; Vernekar et al., 1994; Douville and Royer, 1996). Similar linkages between snow cover and ENSO have also been noted (Groisman et al., 1994; Yang, 1996; Sankar Rao et al., 1996).

To follow the biennial sequence for the south Asian monsoon in Fig. 1b, if the south Asian land area is relatively warm to begin with (right panel of Fig. 1b), this produces enhanced land-sea temperature contrast and a relatively strong monsoon (or a strong convective maximum to use the terminology from the atmosphere-ocean biennial discussion above). The strong monsoon is associated with greater precipitation, higher evaporation and stronger winds from the Indian Ocean, and elevated land surface moisture (top panel of Fig. 1a). At the end of the strong monsoon, the saturated land surface produces greater latent heat flux and contributes to relatively cool temperatures over land. If these cool land temperatures can persist for one year (left panel of Fig. 1b), reduced land-sea temperature contrast is set up to contribute to a relatively weak monsoon the following year (bottom panel of Fig. 1b). The weak monsoon is associated

with less precipitation, lower evaporation from the Indian Ocean and weaker low level inflow. The reduced precipitation does not saturate the land surface, latent heat flux is not as high, and the land surface is left relatively warm at the end of the weak monsoon season. If these relatively warm land surface temperatures can persist for one year (right panel of Fig. 1b), enhanced land-sea temperature contrast sets up a relatively strong monsoon during the next northern summer, and so on.

3. Observations

As noted above there are well-known links between the south Asian monsoon and the SO (e.g. Webster and Yang, 1992; Yasunari and Seki, 1992; Ju and Slingo, 1995). Rasmusson and Carpenter (1983) showed that for roughly a one hundred year period, there were 25 warm events in the Pacific and 21 of those had Indian monsoon rainfall below normal. Meehl (1987) used relatively strong and weak Indian monsoons to show associated signals in the Pacific Ocean that resembled those of cold and warm events, respectively, and that SST anomalies in the tropical Indian and Pacific Oceans varied in phase. These links between the Indian monsoon, Indian Ocean, and the tropical eastern Pacific were shown to have a biennial tendency in that study, and those results have been reconfirmed in subsequent analyses.

For example, Figures 2 and 3 show precipitation and surface temperature anomalies for warm minus cold event composites (after Kiladis and Van Loon, 1988). In the season MJJ-1 in Fig. 2a (the May-June-July season prior to a warm event or, for the monsoon, prior to a weak monsoon) many areas in the south Asian monsoon region show excess precipitation (as in the top panel of Fig. 1b). Associated with the strong monsoon the land temperatures decrease in Fig. 3a. By the end of the strong monsoon season (Fig. 3b) the land temperatures over most of south Asia are below normal. These conditions over south Asia then persist through winter (Fig. 3c) into spring (Fig. 3d).

This corresponds to the left panel in Fig. 1b. These land temperature anomalies vary in phase with tropical Indian Ocean SSTs and eastern Pacific SSTs (Meehl, 1987).

During the northern winter, precipitation anomalies in the tropical Pacific and Indian Ocean areas follow the conceptual model in Fig. 1a. That is, a relatively strong convective maximum moves over the relatively warm waters in the Australasian region (Fig. 3b and c) with the seasonal cycle. The strong convective maximum in Fig. 2b is manifested as positive precipitation anomalies in the seasonal rainfall areas of Australasia. In response, SSTs cool and are left relatively low to the north and west of the convective maximum as also described by Meehl (1987, 1993). The large-scale east-west circulation is playing a role in the Australasian sector with increased vertical motion and upper level outflow, and suppressed convection over the western Indian Ocean and eastern Pacific in association with cool SSTs in those regions. Just out of the picture in Fig. 2c are positive precipitation anomalies over central Africa also involved with the large-scale east-west circulation in the atmosphere (see also Kiladis and Diaz, 1989; Halpert and Ropelewski, 1992; Ropelewski and Halpert, 1987; Lau, 1992).

The relatively cold land temperatures over south Asia during northern winter and spring set up decreased land-sea temperature contrast and contribute to a weak Indian monsoon the following summer in Fig. 2c (as also noted in Fig. 1b, bottom panel). The reduced precipitation amounts are then associated with a warmer, relatively drier land surface, and positive surface temperature anomalies are left at the end of the monsoon season (Fig. 3f). These conditions then persist through the rest of the year (Fig. 3g and h, corresponding to the right panel of Fig. 1b) to set up enhanced land-sea contrast for the following strong monsoon season, and so on. Note in Fig. 2d that the weak convective maximum that has moved over Australasia with the seasonal cycle is associated with reduced precipitation amounts in that region, and relatively warm SSTs are left to the north and west of the convective maximum. Also note in Fig. 2d that the weak con-

vective maximum in Australasia is part of the large-scale east-west circulation such that elevated precipitation amounts are occurring to the west over the eastern Indian Ocean and over the eastern Pacific. Kiladis and Diaz (1989) also note enhanced precipitation over continental Africa in association with these alterations of the east-west circulation.

A further documentation of observed variability of precipitation in the global tropics has been performed by Lau and Sheu (1988). Fig. 4a shows the pattern of the first EOF of the monthly mean precipitation from their analysis of station precipitation data. This EOF explains 9% of the variance of the station precipitation data. The pattern reflects features of precipitation variability discussed above. When precipitation is above normal in the Indian monsoon region, it is also above normal over the rest of Australasia, and below normal over the eastern Pacific and central Africa. Spectra of this leading EOF show a biennial peak at a little more than 2 years, as well as a peak associated with the SO at about 5-6 years (Fig. 4b).

4. Coupled Model Analysis

In this section we use a coarse-grid global coupled ocean-atmosphere GCM to study the processes postulated above for the observed climate system. This model has been shown to represent many of the aspects of the observed large-scale mean climate (Washington and Meehl, 1989), climate variability compared to satellite observations (Meehl et al., 1994), and some aspects of ENSO (Meehl, 1990). Variability of the simulated south Asian monsoon has been shown to resemble the observed monsoon as well (Meehl and Washington, 1993).

Details of the model are described elsewhere (Washington and Meehl, 1989). Briefly, the model uses a global spectral rhomboidal 15 (R15, roughly 4.5 degrees latitude, 7.5 degrees longitude) 9 level spectral atmospheric GCM. The atmospheric model is coupled to a global coarse-grid (5 x 5) 4 layer ocean GCM. The sea ice is a simple thermodynamic formulation. The atmospheric model was spun up for 25 years with a 50 m deep non-dynamic slab mixed layer. The ocean was initialized with observed cross-sections of temperature and salinity and then run with observed atmospheric surface temperatures and wind stress for 50 years. The models were then coupled together and an integration was performed without flux correction for present-day climate for 70 years. The analyses presented here will use the last 50 years of that integration.

An EOF analysis is performed on the detrended monthly mean time series of precipitation. The seasonal cycle is removed by subtracting the first three harmonics from the time series (for details see Campbell et al, 1994). The first two EOFs from the model are very similar, and both show features present in the observed pattern in Fig. 4a. The first EOF explains 3.1% of the variance, while the second explains 2.6% for a combined total of 5.7% of the total variance (compared to 9% of variance for the first EOF from observed precipitation in Fig. 4a). Though these explained variance numbers are low for the model and observations due to the noisy nature of precipitation data, the leading EOF patterns are instructive for understanding possible physical processes. The first two EOFs from the coupled model both show an opposition of sign of precipitation variability between the equatorial central Pacific and areas of south Asia, south Africa, west Africa, northern Australia and northern South America (see also for the observations in Fig. 4a). Both also show agreement of sign between the central equatorial Pacific and equatorial east Africa. This pattern can readily be seen in EOF2 from the model and is plotted in Fig. 4c. In the model (as in the observed) there is a dipole over south Asia with an opposition of sign between India and southeast Asia. The power spectrum for this EOF is shown in Fig. 4d. As in the observed, there is a biennial peak at about 2.3-2.4 years, as well as an ENSO peak near 4-6 years.

To examine timescales of variability in monsoon observations, spectra are computed for 50 years of an observed Indian monsoon index (Parthasarathy et al., 1991)

and compared to similar spectra from the coupled model for rainfall averaged over India (land points only from 5N-30N, 65E-95E). The 1901-1950 period had a particularly active biennial cycle and the observed time series shows a peak significant at the 95% level at the quasi-biennial timescale of 2.3 years in Fig. 5a. Similar spectra for the 50 year time series of JJA rainfall from the coupled model also show a biennial peak at 2.3 years. Both the observed and model monsoon time series also show peaks associated with ENSO. For the observed there is a peak at 3.3 years, and for the model at 4.5 years. The model biennial peak in Fig. 5b is below the 95% significance level indicating that the biennial amplitude is less than the observations. This lower amplitude variability in the coupled model compared to observations is consistent with other aspects of tropical interannual variability that have amplitudes less than the observed (e.g. Meehl, 1990; Meehl and Washington, 1993; Meehl et al, 1994) and in other coupled models of this class (e.g. Latif et al., 1994).

It was noted earlier that the south Asian monsoon has a strong link to the ENSO cycle. For the coupled model, during the 50 year period of analysis there were 8 warm events in the Pacific (defined as the Nino3, 10N to 10S and 90W to 150W, area-averaged SST anomalies greater than 0.25C, roughly one standard deviation) and 5 of those had Indian monsoon precipitation below normal. For 9 cold events during that 50 year period in the model, (Nino3 SST anomalies less than -0.25C) there were 6 Indian monsoons above normal. If the definition basis is the monsoon, for 10 Indian monsoons with area-averaged precipitation above one standard deviation, the SSTs in the Nino3 area were below normal 7 times. For 11 Indian monsoons with precipitation greater than one standard deviation, Nino3 SSTs were above normal 7 times. As another measure of the connections between the tropical Pacific and Indian sectors in the coupled model, sea level pressure over the Indian Ocean and Nino3 SSTs have a correlation coefficient of +0.54 which is significant at the 5% level. This linkage is also seen in the EOFs of pre-

cipitation from the coupled model in Fig. 4 where there is an opposition of sign between precipitation in the Indian monsoon and the eastern equatorial Pacific in both EOF1 (not shown) and EOF2 (Fig. 4c). Both EOF1 and EOF2 have biennial peaks, while EOF2 has the stronger ENSO time scale peak (Fig. 4d). Therefore we conclude that the Pacific-monsoon links in the model exist, but are not as strong as in the observed system. Again this is consistent with evidence cited above that coupled variability in the tropics in the model is weaker than observed, and this seems to be reflected in terms of east-west circulation links as well.

In Fig. 6a the evolution of various elements of the monsoon system in relation to a strong monsoon are shown schematically as summarized from the observed sources cited in the Introduction and configured to conform to the conceptual model shown in Fig. 1b. As noted above, for the northern winter and spring seasons prior to a strong monsoon there is a tendency for Asian land temperatures to be above normal (solid line in Fig. 6a) contributing to enhanced land-sea temperature contrast. The Indian Ocean SSTs (dash-double-dot line) are also above normal but the land temperatures are proportionately higher. This maintains enhanced land-sea temperature contrast with the positive SST anomalies over the Indian Ocean contributing to elevated evaporation levels. The warm south Asian land temperatures are then associated with less snow cover over south Asia (bars in Fig. 6a). During the strong monsoon season with monsoon precipitation above normal (dashed line), the south Asian land temperatures drop along with Indian Ocean SSTs. These conditions persist through the next northern fall, winter, and spring contributing to increased snow cover, decreased land-sea temperature contrast, and a subsequent weak monsoon the following northern summer. The connection to the tropical Pacific is shown in terms of Nino3 SSTs that are below normal the northern spring before the strong monsoon, and then transition to above normal the northern spring before a weak monsoon.

To examine the proposed processes involved with the coupled land-atmosphere-ocean mechanism in Fig. 1b, various area averages are computed from the coupled model. Asian monsoon precipitation and soil moisture are computed as the average of land points in the area 5N-40N, 60E-100E. South Asian land temperatures area are calculated for land points in the area 2N-30N, 70E-120E. Asian snow cover is liquid water equivalent over the area 20N-70N, 50E-130E. Indian Ocean SST is from ocean points in the area 5S-30N, 50E-100E. Australian monsoon precipitation is computed for all points in the area 25S-Eq., 100E-150E. Nino3 SST is computed for the area 10S-10N, 150W-90W.

These area averages are composited as in Meehl (1987, 1993) based on an index of area-averaged Indian monsoon rainfall. This index is formed by averaging all land points over the Indian region in the model as noted above. From this time series extreme wet or dry monsoons (in excess of one standard deviation) for the JJA season from the model are used to compute area averages for various other parameters, and differences are computed for strong minus weak monsoons. These differences are plotted as a function of season in Fig. 6. Maximum magnitudes of these differences are about 5 to 20% of the strong or weak monsoon averages and in most cases are around one standard deviation of the monsoon seasonal values. The sign of the differences is that of a strong monsoon, the calendar year of the strong monsoon is designated year 0, and the seasons preceding and following the strong monsoon follow that convention.

For the coupled model in Fig. 6b, there are a number of similarities to the schematic representation of the observed system in Fig. 6a. In particular, south Asian land temperatures are elevated in the northern winter and spring before a strong monsoon in relation to Indian Ocean SSTs to produce decreased land-sea temperature contrast. This is associated with reduced Asian snow cover. During the JJA season of a strong monsoon, the south Asian land temperatures decrease as soil moisture amounts increase due to the heavy rainfall. The cool south Asian land temperatures persist through the

following northern fall, winter and spring seasons to contribute to enhanced land-sea temperature contrast and a relatively weak monsoon the following JJA. The cool south Asian land temperatures are also associated with increased south Asian snow cover during northern winter and spring.

In the discussion of Fig. 1 it was noted that the ocean heat content provides the one year timescale memory for the persistence of the observed SST anomalies. The question was also raised as to how a similar memory could exist over a land surface with virtually no heat capacity. It is possible that surface hydrology could accomplish this if, for the case of a strong monsoon, the land surface could remain saturated for the duration of the year following a strong monsoon. In that way elevated latent heat flux would contribute to a cold land surface and the decreased land-sea temperature contrast needed for the following weak monsoon. This could be important in light of the previously recognized role of evapotranspiration in climate variability (e.g. Shukla and Mintz, 1982).

In the coupled model in Fig. 6b it can be seen that elevated soil moisture levels, (with corresponding increases of latent heat flux, not shown), occurring in conjunction with the strong monsoon in JJA0, persist into northern fall (SON0). But by the following northern winter the soil moisture differences are near zero. Additionally, those differences are also near zero prior to a strong monsoon. It would appear that surface hydrology plays a role in contributing to land surface temperature anomalies for only part of the year. Consequently, other processes must be at work to maintain south Asian land surface temperature anomalies on the one year timescale.

5. Tropical Forcing of Midlatitude Circulation

The question before us now is what is causing the persistence of south Asian land surface temperature anomalies with a one year timescale that contributes to setting up land-sea temperature contrast in the TBO? It would appear that some other forcing,

possibly from remote sources, could be important.

Evidence has been presented in previous studies of the role of tropical convective heating anomalies in forcing anomalous midlatitude circulation via remote Rossby wave response (e.g. Branstator, 1983; Branstator 1990; Ting, 1994), and that such forcing could affect tropical and extratropical circulation having to do with the monsoon (Yasunari and Seki, 1992; Nigam, 1994; Ting, 1994). These studies and others (e.g. Barnett, 1988; Chen and Yen, 1993,1994) have shown the possibility of connections between the tropics and midlatitudes involving the south Asian monsoon. Perhaps heating from anomalous convection associated with the coupled air-sea biennial mechanism summarized in Fig. 1a and documented by Meehl (1987, 1993) could be altering the midlatitude circulation in such a way as to contribute to the persistence of the surface temperature anomalies over south Asia.

To investigate this hypothesis surface temperature and 500 mb height anomalies from the coupled model, strong minus weak monsoons, are calculated and shown in Fig. 7a,b for the DJF season prior to a strong monsoon (DJF0 in Fig. 7). Area-averaged interannual standard deviations from the model over south Asia are roughly 1.0C for surface temperature and about 20m for 500 mb height. As noted in Fig. 6, temperature differences are positive over south Asia. These are separated from the positive differences over north Asia by small negative values over central Asia. The 500 mb height differences are shown in Fig. 7b. There is a well-organized large-scale pattern with negative differences over the Mideast, positive differences of over 35m over north Asia, and negative differences over northeast Asia. This is indicative of a midlatitude longwave pattern such that there is anomalous ridging over Asia. Such a pattern would contribute to maintaining relatively warm surface temperatures over south Asia via southerly advection of warm air under the ridge as illustrated, for example, by van Loon and Williams (1977).

To compare these model results to recent observations, surface temperature differences from the ECMWF analyses (for description see Trenberth, 1992) for the northern winter 1988 (i.e. December 1987, January, February 1988) minus 1987 are shown in Fig. 7c. The 1988 monsoon season was strong, and 1987 was a weak monsoon (e.g. Krishnamurti et al., 1989; Krishnamurti et al., 1990). Therefore, the 1988 minus 1987 northern winter differences have the sign of conditions prior to a strong monsoon. Similar to the coupled model composites in Fig. 7a, positive differences of +2C to +3C occur over most of south Asia and north Asia with negative differences over central Asia. Most of Africa is covered by positive differences as well. Associated with these surface temperature differences are the 1988 minus 1987 DJF 500 mb height differences in Fig. 7d. Also similar to the coupled model, negative differences are located over the Mideast with positive differences over north Asia and negative differences over east Asia signifying anomalous ridging over Asia in the winter prior to the strong monsoon year (1988) compared to the winter prior to the weak monsoon year (1987).

To test the hypothesis that anomalous heat sources associated with tropical convective anomalies are associated with the anomalous 500 mb circulation and surface temperature anomalies, a global atmospheric GCM is run in perpetual January mode with specified climatological SSTs and anomalous heat sources and sinks. The heat sources corresponding to positive precipitation anomalies are centered at 30E, Equator over continental Africa, and at 160E, Equator over the Pacific, with an anomalous heat sink (corresponding to negative precipitation anomalies) at 130E, Equator. These heating anomalies roughly correspond to centers of precipitation maxima and minima in EOF 1 from the observed precipitation analysis of Lau and Sheu shown in Fig. 4a, and also match observed northern winter precipitation anomalies from the Kiladis and van Loon analysis in Fig. 2d as well as similar anomalous precipitation maxima shown by Meehl (1987) for the tropical Pacific. The coupled model EOF2 suggests similar anomalous

heating over east Africa (see Fig. 4c). The EOF2 precipitation variability center is farther east in the Pacific, but EOF1 (not shown) has this center shifted farther west.

The anomalous heating in the GCM is specified as in Branstator (1990) and Meehl et al. (1993). The heating is sinusoidal in the vertical with a mid-tropospheric maximum of 5C. The heating decreases linearly away from the central point in all directions to a radius of 1500 km. Figures 7e and f show differences for the perpetual January integration, the 795 day average (days 100-895) from the experiment minus a 2700 day average (days 100-2800) from the control integration. Standard deviations are similar in magnitude to the coupled model. Surface temperature differences in Fig. 7e show large coherent warming of about +2C to +5C over most of Africa and Asia in rough agreement with the coupled model in Fig. 7a and the observations in Fig. 7c. The associated 500 mb height difference map in Fig. 7f shows a similar pattern as well with negative differences over the Mideast, positive values of around 60m over north Asia, and negative values over east Asia. The results from this sensitivity experiment suggest that anomalous heating from convective anomalies in the tropics associated with the coupled atmosphere-ocean biennial mechanism can produce changes in the midlatitude circulation such that the south Asian land surface temperature anomalies are maintained by anomalous heat transport caused by shifts in the midlatitude longwaves and associated changes in advection (e.g. van Loon and Williams, 1977).

To further examine this possibility, surface temperature differences for the northern winter season following a strong monsoon (DJF+1) and preceding a weak monsoon from the coupled model are shown in Fig. 8a. As noted in Fig. 6 for this season, surface temperature differences over south Asia are negative with values around -0.5C to -1.0C. Additionally, surface temperatures are cool over north Asia and much of continental Africa. The associated 500 mb height anomalies in Fig. 8b for DJF prior to a weak monsoon show almost the opposite pattern to that in Fig. 7b for the DJF season preceding a strong monsoon. Namely, positive anomalies lie over the Mideast and central Asia with negative values of nearly -20m over north Asia with positive anomalies over east Asia.

The observations for the 1989 minus 1988 DJF season in Figs. 8c and d, corresponding to the period following the strong 1988 monsoon, show a similar pattern. Most of south Asia and Africa is relatively cool in Fig. 8c with values around -1C to -4C, and the 500 mb height differences in Fig. 8d show positive values over the eastern Mediterranean and Mideast with negative values over north Asia and positive differences over east Asia.

The perpetual January GCM experiment is next configured to have the opposite anomalies to that for the experiment in Figs. 7e and f to represent precipitation anomalies for the northern winter following a strong monsoon. Negative heating anomalies (representative of suppressed convection and thus a heating deficit) are centered at 30E, Equator and 160E, Equator, with a positive heating anomaly at 130E, Equator. Surface temperature differences computed as described above for Fig. 7e appear in Fig. 8e and show that surface temperatures are cooler over much of south Asia and Africa with values of about -2C to -6C. The 500 mb height anomaly pattern in Fig. 8f also shows agreement with Fig. 8b and d in that there are positive values over the eastern Mediterranean and Mideast, negative values of about -70m over north Asia, and positive values over east Asia indicative of a shift in the longwave pattern with an anomalous Asian trough with associated cold air advection over south Asia.

A number of other sensitivity experiments were carried out with anomalous equatorial heating and cooling centers shifted to various other longitudes to represent other features noted in the observed and model-simulated precipitation EOFs. In general, the African heating anomaly in concert with either the Indonesian and/or the western

Pacific anomaly could produce the appropriate circulation anomalies over Asia. However, the combinations shown here involving heating/cooling anomalies over the Pacific/Australasia and Africa produced the best match to the coupled model and observed mid-latitude response over Asia. This points to the role of African precipitation anomalies (see Hastenrath et al., 1993 for discussion of east African precipitation regimes) acting in combination with convective heating anomalies over the western Pacific in contributing to midlatitude conditions conducive to subsequent Indian monsoon development.

This analysis shows that by placing tropical convective heating anomalies in a perpetual January version of a GCM, patterns similar to those seen in the 1987-88-89 sequence of years prior to and following the strong monsoon of 1988 can be reproduced. The question is, are there precipitation anomalies in the coupled model or in the observations that correspond to these convective heating anomalies? To address that question we compute area-averaged precipitation anomalies from the coupled model and outgoing longwave radiation (OLR, taken as a proxy for precipitation) for the northern winter of 1988 minus 1987 to illustrate conditions prior to a strong monsoon, and for 1989 minus 1988 for conditions after a strong monsoon (Table 1). In the coupled model for DJF0, the positive precipitation anomalies over east Africa and the western Pacific are +0.35 mm day^{-1} and +0.24 mm day^{-1}, respectively, and are consistent with positive convective heating anomalies in those regions. The Australian monsoon precipitation anomalies are near zero. Thus two of the three areas (the two positive heating anomalies) are consistent with the optimum specified heating anomaly pattern in Fig. 7e,f. For the coupled model DJF+1 season, negative precipitation anomalies exist over east Africa and the western Pacific (-0.24 mm day^{-1} and -0.08 mm day^{-1} respectively) with positive anomalies over the Australian monsoon region (+0.36 mm day^{-1}). These anomalies are consistent with convective heating anomalies in the DJF+1 case in

Fig. 8e,f. For the OLR observations for DJF0 (1988 minus 1987), the east Africa and Australian monsoon areas are consistent with the heat sources and sinks in the atmospheric GCM specified heating experiments. Negative OLR anomalies (indicating intensified convection and precipitation) of -3.46 W m^{-2} in DJF0 are present over east Africa, with positive OLR anomalies (indicative of suppressed convection and less precipitation) over the Australian monsoon (+9.95 W m^{-2}). Anomalies of opposite sign are present in those areas for the DJF+1 season following the strong monsoon (+5.67 W m^{-2} and -6.67 W m^{-2}, respectively). The signal is not consistent in the Pacific for the DJF0 season (+1.38 W m^{-2}), but does go along with the composite picture in DJF+1 with an area averaged anomaly of +2.61 W m^{-2} indicative of suppressed convection. These results are consistent with the specified convective heating anomaly experiments in that some combination of convective heating anomalies over Africa and the western Pacific is likely to be important for the appropriate response of the midlatitude longwave pattern over Asia.

6. The March-April-May Season

So far we have focused on the DJF SST and convective heating anomalies and their association with anomalous circulation over the Asian continent. This circulation, if persistent, could set up conditions that would affect the subsequent monsoon season. Ju and Slingo (1995), Soman and Slingo (1996), and Tomita and Yasunari (1996) have pointed to the importance of SST and associated convective heating anomalies in the northern spring season over the southeast Asian region in setting up conditions for either a strong or weak south Asian monsoon the following summer. Meehl (1987, 1993) noted that the northern spring season is a time of transition for SST anomalies in the tropical Pacific region in the TBO cycle. As shown in Fig. 6a, observed Nino3 SST anomalies tend to change sign going from DJF0 to MAM0, thus also changing the pattern of associated convective heating anomalies in the western Pacific. Could the midlatitude circu-

lation patterns over Asia, set up by convective heating anomalies in the DJF0 season, be maintained through the MAM0 season with a different set of SST and associated convective heating anomalies as noted, for example, by Ju and Slingo (1995) and Soman and Slingo (1996).

To give a preliminary idea as to whether this is a possibility, the specified convective heating anomaly version of the atmospheric GCM is run to provide an analog to the MAM season in two additional experiments. As indicated by Meehl (1987, 1993) and noted by Ju and Slingo (1995) and Soman and Slingo (1996), conditions in the Pacific region in the MAM0 season (prior to a strong south Asian monsoon) involve relatively warm SSTs over Indonesia and north of Australia (left that way by the weak Australian monsoon during DJF0), while the tropical Pacific SST anomalies transition from relatively warm to relatively cool (see also Fig. 6a). Therefore, in association with those SST anomalies, during MAM0 there should be somewhat stronger convection over the Indonesia area compared to that over the western tropical Pacific. To represent these conditions, an anomalous heat source is placed at 120E, Equator in the atmospheric GCM. The results shown in Fig. 9a show an anomalous ridge over Asia and positive land surface temperature anomalies similar to that seen for DJF0 in Fig. 7e and f. This pattern would be associated with weakened tropospheric westerlies over south Asia that have been shown in observations to be associated with a strong monsoon the following summer (e.g. Yang and Webster, 1990; Webster and Yang, 1992; Yasunari and Seki, 1992; Ju and Slingo, 1995; Soman and Slingo, 1996; Tomita and Yasunari, 1996).

Conversely, for the MAM+1 season following a strong monsoon and preceding a weak monsoon, Nino3 SSTs transition from anomalously cool to anomalously warm (Fig. 6a), while SSTs over Indonesia and north of Australia have been left anomalously cool after the relatively strong Australian monsoon. Thus a convective heating anomaly placed at 150W, Equator in the region of anomalously warm SSTs in the tropical Pacific

is associated with an anomalous trough over Asia (Fig. 9c) and relatively cold land surface temperatures there as well (Fig. 9d). This would result in anomalously strong mid-tropospheric westerlies over south Asia prior to a weak monsoon as noted in observations prior to a weak monsoon (Yang and Webster, 1990; Webster and Yang, 1992; Yasunari and Seki, 1992; Ju and Slingo, 1995; Soman and Slingo, 1996; and Tomita and Yasunari, 1996).

Similar patterns for the coupled model and the 1987-88-89 sequence for the MAM seasons (not shown) seem to suggest that even though the SST anomaly patterns and associated convective heating anomalies in the tropics transition to different locations going from DJF to MAM, the contribution of the convective heating anomalies to the midlatitude circulation anomalies is still such that the pattern from the preceding DJF season could persist through MAM and thereby maintain the DJF conditions to set up the following monsoon season. A more rigorous examination of the transitions that occur during the MAM season is currently being formulated.

7. Links to Other Regions

Several key points have emerged from the previous analysis of mechanisms involved with the TBO and the Indian monsoon. First, a large part of the global tropics appear to be involved (see also Ward, 1995) and, in particular, African precipitation anomalies may play a role in helping to set up the midlatitude circulation in conjunction with convective heating anomalies in the western Pacific and Australasia. Second, the patterns of precipitation anomalies involved with the TBO also appear to be involved in a similar way with the Southern Oscillation. This was essentially what was postulated by Meehl (1987) such that excursions of the TBO are manifested as extremes in the Southern Oscillation. Consequently, anomalies in the climate system in various other regions that are associated with the Southern Oscillation (and by extension the TBO)

can be examined to look for similar connections.

It has been noted above that anomalously warm SSTs in the tropical Pacific are often associated with a weak south Asian monsoon. Barnett et al. (1989) used model results to suggest that the remote response from a weak south Asian monsoon could be to enhance warm SST anomalies in the tropical Pacific via surface wind stress anomalies directly forced by the weak monsoon. To further address this issue here, we show surface vector wind anomalies (Fig. 10) from a weak south Asian monsoon sensitivity experiment (induced by increasing land albedos in the atmospheric GCM–see full description of the experiment by Meehl, 1994b). SSTs in this sensitivity experiment do not change. The surface wind response in the Indian region shows anomalous northeasterlies as expected in association with the weakened monsoon southwesterly flow (for full wind field see Meehl, 1989). However, in the tropical Pacific there are westerly surface wind anomalies of around 1 m sec^{-1} (about 15%). Such westerly surface wind anomalies would be conducive to weakened upwelling, reduced latent heat flux, and advection of western Pacific warm pool surface water to the east. All of these processes would contribute to positive SST anomalies in the equatorial Pacific. Thus the model results indicate that a weak monsoon can independently produce surface westerly wind stress anomalies in the equatorial Pacific via the large-scale east-west atmospheric circulation. These wind anomalies can contribute to SST anomalies in the tropical Pacific, thus confirming the earlier Barnett et al. (1989) results and emphasizing the active role of the south Asian monsoon in the TBO.

Due to the linkage of the Indian monsoon to African precipitation, several additional area averages relating to precipitation anomalies over regions of Africa are calculated. Nicholson (1996), Lamb and Peppler (1991) and others have documented factors that are associated with African precipitation anomalies. Lamb and Peppler (1991) note that strong Sahel rainfall is often associated with a weak subtropical high in the north

Atlantic, a strong subtropical high in the south Atlantic, and a northward shift and intensification of precipitation over west Africa and the Sahel. The two contrasting west African monsoon seasons of northern summer 1987 (weak) and 1988 (strong) suggest a link to the 1987 Indian monsoon (weak) and the 1988 Indian monsoon (strong). Consistent with these associations, area averages from the coupled model show that, on average, anomalously high Sahel precipitation (+1.02 mm/day over the area 10N - 20N, 20W - 10E) is associated with strong Indian monsoons along with a weakened subtropical high in the north Atlantic (-0.3 mb over the area 20N - 40N, 70W - 10W). The opposite is the case for the year following a weak Indian monsoon (Sahel rainfall anomalously low at -0.45 mm/day and the north Atlantic subtropical high stronger at +0.7 mb). Lamb and Peppler (1991) and others have also shown that the south Atlantic high is relatively weaker during years of deficient Sahel rainfall, and stronger during years of abundant Sahel rainfall. In the coupled model the south Atlantic high shows negative anomalies for both strong and weak Sahel rainfall years suggesting that the signal is not consistent in this region of the model.

Nicholson (1996) shows that anomalously warm SSTs in the tropical eastern Pacific are often associated with warm SSTs in the Indian Ocean (also shown by Meehl, 1987) as well as warm SSTs in the equatorial Atlantic south of about 10N. Such an SST pattern has been shown by Lamb and Peppler (1991) and others to be associated with a reduction of Sahel rainfall. The coupled model shows that when Sahel precipitation is strong in the year of a strong Indian monsoon, equatorial Atlantic SSTs are lower by -0.20 C over the area 20S - 10N, 35W - 10W, while the following year when Sahel precipitation is weaker, the Atlantic SSTs are warmer at +0.07 C.

Previous associations of the monsoon with Southern Hemisphere circulation have shown that a strong Indian monsoon is often associated with stronger subtropical highs in the southern Indian and Pacific Oceans, while the opposite is the case for a weak In-

dian monsoon (e.g. Meehl, 1987, 1988; Clemens and Oglesby, 1992). This is also the case in the coupled model with area averaged sea level pressure in the subtropical high regions of the south Indian (20S - 40S, 60E - 100E) and south Pacific (20S - 40S, 90W - 150W) Oceans during the JJA0 season at +0.4 mb and +0.5 mb respectively. The year following a relatively weak Indian monsoon, these two subtropical highs are also weakened at -0.1 mb and -0.4 mb respectively.

South African precipitation during southern summer has also been shown to be related to SSTs in the tropical Pacific. Kiladis and Diaz (1989) show deficient south African precipitation during years of warm SSTs in the tropical eastern Pacific prior to a strong Indian monsoon. This is also the case in the coupled model as was demonstrated first by Meehl et al., (1993) and also shown here. In the southern summer prior to a strong Indian monsoon south African precipitation is deficient in the coupled model (-0.60 mm/day over the area 40S - 20S, 10E - 50E), while for southern summers following a strong Indian monsoon South African precipitation anomalies are positive (+0.49 mm/day).

Other studies have also linked Pacific SSTs to precipitation over northern South America (e.g. Kiladis and Diaz, 1989; Ropelewski and Halpert, 1987, 1989; Marengo and Hastenrath, 1993). Meehl et al. (1993) showed this linkage for ENSO-like events in the coupled model. But for the monsoon definition base used here, that association is not consistent with deficient south American rainfall both prior to and after a strong Indian monsoon.

8. Conclusions

The tropospheric biennial mechanism (TBO) involving atmosphere-ocean coupled processes postulated by Meehl (1987, 1993, 1994a) is reviewed. Premises involving dependence on the seasonal cycle of convection being strong during one season of the year

at any given location in the Indian and Pacific sector, air-sea coupling being strongest during that season, and upper ocean heat content providing the memory to maintain SST anomalies for one year are all shown to have some basis in observations. The sign of South Asian land temperature anomalies, and tropical Indian and eastern Pacific SST anomalies all vary roughly in phase within about a season over the duration of the seasonal cycle beginning in about June.

It is noted that earlier studies of the TBO showed a connection with the south Asian or Indian monsoon, but it was unclear whether the monsoon was an active or passive participant. A biennial mechanism involving coupled atmosphere-land-ocean interactions is postulated that involves the monsoon as an active participant in the TBO.

A 50 year time series from a global coupled ocean-atmosphere GCM is analyzed to look for evidence of this proposed mechanism. The simulated monsoon is shown to have links to the model's version of ENSO in the Pacific not unlike the observed system, but the amplitude of the variability and thus the strength of those linkages is weaker than in the observations.

Results from the coupled model for strong minus weak monsoon years demonstrate similarity to the observed relationships in terms of the biennial mechanism. However, since the soil moisture anomalies that occur in conjunction with heavy rainfall during a strong monsoon only last for one additional season, it is suggested that remote processes, not local hydrology, must be contributing to maintaining anomalous land temperatures over south Asia on a one year timescale. It is hypothesized that anomalous heat sources and sinks associated with SST and convective anomalies produced by air-sea interaction and east-west atmospheric circulation over the tropical Indian and Pacific sectors involved with the atmosphere-ocean biennial mechanism may be forcing circulation anomalies in the midlatitudes via remote Rossby wave response. Such forcing

could alter the midlatitude circulation in such a way as to maintain the surface temperature anomalies over south Asia (that are essential to the atmosphere-land-ocean biennial mechanism).

To test this hypothesis, a global GCM with specified SSTs as well as static soil moisture and snow cover is run in perpetual January mode with heat sources and sinks specified to correspond to key precipitation anomalies in the coupled model, as well as to conform to heating anomalies suggested by the first EOF of observed tropical precipitation and similar patterns from other observed studies. It is found that by specifying a combination of heat sources and sinks over Africa and the western Pacific Ocean, anomalous surface temperature signals over Asia resemble those from the coupled model as well as from the ECMWF analyses from a recent weak to strong monsoon evolution (1987 to 1988). An additional GCM simulation with specified climatological SSTs shows that westerly surface wind anomalies in the equatorial Pacific develop as a direct consequence of a weak south Asian monsoon induced in a sensitivity experiment. This link between south Asian monsoon strength and conditions that could intensify SST anomalies in the tropical Pacific agrees with previous studies and further points to the active role of the south Asian monsoon in the TBO and ENSO.

Additional precipitation and sea level pressure anomalies are noted from previous observational studies and identified in the coupled model to show the probable near-global nature of the mechanisms involved with the TBO. However, of crucial importance for the monsoon biennial mechanism are the combination of convective heating anomalies over Africa and the western Pacific that has the consequence of involving alterations of the midlatitude circulation over Asia such that subsequent monsoon development is affected.

To summarize the mechanisms involved with the TBO, a schematic evolution of

the features noted in Table 1 and in Figs. 6-9 is shown in Fig. 11. Though associations with rainfall in other parts of Africa, SST and circulation anomalies in the Atlantic, and subtropical SLP anomalies in the Southern Hemisphere have been noted above for the coupled model, we limit this schematic to the strongest associations in the east Africa–India–Pacific sectors. It is likely that the TBO could be characterized as a tropic-wide or even larger scale oscillation (e.g. see Ward, 1995) but in this paper we have chosen to focus on the sectors illustrated in Fig. 11. Year0 and Year+1 indicate calendar years of strong and weak monsoons, respectively. The monsoon seasonal cycle (and also the TBO seasonal cycle as noted by Meehl, 1987) associated with transitions late in northern spring with the beginning of the south Asian monsoon season that is the starting point of a set of seasonally linked anomalies until late the following northern spring (e.g. Meehl, 1987; Yasunari, 1991) is denoted in Fig. 11 by stippling for TBO seasonal cycle 1, and non-stippled for TBO seasonal cycle 2.

Since Fig. 11 depicts an idealized TBO cycle, the staring point for discussion is arbitrary. We choose to begin during northern winter DJF0 before a strong monsoon (at the right side of Fig. 11) when there is relatively heavy rainfall over east Africa and the tropical Pacific, and a weak Australian monsoon. The SST anomaly pattern involves positive values in the Indian and Pacific with negative anomalies north of Australia. The SST and associated convection anomalies have been set up in the previous seasons in the TBO cycle. The tropical convective heating anomalies during DJF0 are associated with a midlatitude longwave pattern with an anomalous ridge over Asia. This ridge is associated with warmer and drier conditions over Asia and thus decreased snow cover.

By the following northern spring season (MAM0, upper right in Fig. 11), the weak Australian monsoon has left SSTs over Indonesia and north of Australia relatively warm, while in the tropical Pacific SSTs have become to relatively cool. Thus, as the ITCZ heads north, there is relatively weaker convection over the Pacific, with somewhat

stronger convection over the Indonesian region. This anomalous convective heating pattern maintains the midlatitude circulation pattern over Asia from the prior DJF season in Fig. 11a with an anomalous ridge, weakened mid-tropospheric westerlies over south Asia, and relatively warm land surface temperatures.

The following monsoon season (JJA0, Fig. 11c) the anomalously warm south Asian land mass has set up enhanced land-sea or meridional tropospheric temperature contrast. This contributes to a strong monsoon, while air-sea interaction produces an anomalous SST pattern with cool SSTs over the tropical Indian and Pacific regions with anomalously warm SSTs over Indonesia and north of Australia. As the seasonal cycle of convection proceeds to the following northern fall (SON0 at upper left in Fig. 11), the relatively strong convective maximum moves south and east with the seasonal cycle, leaving a relatively wet and cool south Asian land mass behind. The enhanced evaporation from the saturated land surface lasts through that season, and by the following northern winter (DJF+1 at left in Fig. 11), a strong Australian monsoon has set up over the anomalously warm SSTs in that region, while the large-scale east-west circulation in the atmosphere contributes to suppressed convection over east Africa and the central tropical Pacific (where SSTs remain anomalously cool). This combination of convective heating anomalies in the tropics is then associated with a midlatitude circulation that includes an anomalous trough over Asia. The associated cold air advection from higher latitudes maintains a cold south Asian land mass with increased snow cover.

In the subsequent northern spring season (MAM+1, lower left in Fig. 11), the SSTs in the tropical Pacific transition to positive anomalies, and the convective maximum is somewhat stronger over that region with suppressed convection over the Indonesia region. These convective heating anomalies contribute to maintaining the midlatitude circulation pattern from the preceding northern winter with an anomalous trough over south Asia and increased midtropospheric westerlies. The anomalously cool south

Asian land temperatures maintain a decreased land-sea or meridional tropospheric temperature gradient that contributes to a weak monsoon the following northern summer (JJA+1 at bottom in Fig. 11). As this weak convective maximum moves south and east with the seasonal cycle over the relatively cool SSTs near Indonesia in the following northern fall (SON+1, lower right in Fig. 11), the weak monsoon the preceding season has left the south Asian land mass relatively dry and warm, and this idealized version of the TBO cycle would continue with conditions the following northern winter as shown at right in Fig. 11.

Of course the TBO cycle depicted in Fig. 11 is not perfectly biennial as noted in other studies and only appears to operate intermittently or in a subset of years (Meehl, 1987; Barnett, 1991; Terray, 1995). However, recent studies have shown that these associations involving midlatitude circulation patterns and monsoon strength are strong enough to be evident in composites of a number of observed strong and weak monsoon years (e.g. Yang et al., 1996).

The role of Asian snow cover appears to contribute positively to the land temperature anomalies. However, the specified heating experiments demonstrate that tropical convective heating anomalies alone can produce circulation patterns over Asia that produce anomalously warm or cold land surface conditions that contribute to land-sea temperature contrast without any feedbacks from snow cover (snow areas and surface moisture are specified and cannot change in that model). For example, for the two contrasting observed monsoon years considered in this paper, spring snow cover over Eurasia was above normal prior to the weak 1987 monsoon, but near normal before the strong 1988 monsoon even though Eurasian surface temperature anomalies were below normal before the 1987 monsoon and above normal prior to the 1988 monsoon (Halpert and Ropelewski, 1991). Therefore, changes of snow cover appear to be in part an artifact of the midlatitude circulation pattern associated with convective heating anomalies rather than

an independent forcing.

The northern spring season is important for a number of reasons. This is the beginning of the time of transition for SST anomalies in the tropical Pacific as shown in Fig. 6a and Fig. 11. This transition appears to be necessary for the establishment of convective heating anomalies that could help maintain the midlatitude circulation pattern over Asia and thus contribute to subsequent monsoon development. It is likely that the northern spring season transition must occur or the TBO cycle breaks down. Perhaps this is why the northern spring season is problematic for forecasting many features in the tropical Indian-Pacific region and is sometimes referred to as the "spring predictability barrier" (e.g. Webster and Yang, 1992; Lau and Yang, 1996). The mechanisms of this transition involve ocean dynamics and coupled air-sea interaction in the tropical Pacific and well as features of the large-scale east-west circulation in the atmosphere involving the TBO. Future analyses will aim to describe more fully this transition as well as the role of tropical forcing of the extratropical circulation and the interaction of processes over various other regions of the globe that produce the TBO.

Acknowledgements

The author thanks Grant Branstator and Andrew Mai for collaboration on the specified heating experiments. A portion of this study was supported by the Office of Health and Environmental Research, U.S. Department of Energy, as aprt of its Carbon Dioxide Research Program. The National Center for Atmospheric Research is sponsored by the National Science Foundation.

REFERENCES

Alexander, M.A., and K.M. Weickmann, 1995: Biennial variability in an atmospheric general circulation model. *J. Climate*, **8**, 431–440.

Barnett, T.P., 1988: Variations in near-global surface pressure. Another view. *J. Climate*, **1**, 225–230.

Barnett, T.P., 1991: The interaction of multiple time scales in the tropical climate system. *J. Climate*, **4**, 269–285.

Barnett, T.P., L. Dümenil, U. Schlese, E. Roeckner, and M. Latif, 1989: The effect of Eurasian snow cover on regional and global climate variations. *J. Atmos. Sci.*, **46**, 661-685.

Blanford, H.F., 1884: On the connexion of Himalayan snowfall and seasons of drought in India. *Proc. Roy. Soc. London*, **37**, 3-22.

Branstator, G. W., 1983: Horizontal energy propagation in a barotropic atmosphere with meridional and zonal structure. *J. Atmos. Sci.*, **40**, 1689-1708.

Branstator, G. W., 1990: Mechanisms affecting the midlatitude atmospheric response to equatorial heating anomalies. *Proceedings of the TOGA International Scientific Conference*, Honolulu, HI, 16-20 July 1990, WMO Geneva.

Brier, G.W., 1978: The quasi-biennial oscillation and feedback processes in the atmosphere-ocean-earth system. *Mon. Wea. Rev.*, **106**, 938-946.

Campbell, G.G., T.G.F. Kittel, G.A. Meehl, and W.M. Washington, 1995: Low-frequency variability and CO_2 transient climate change. Part 2: EOF analysis of CO_2 and model-configuration sensitivity. *Global and Planetary Change*, **10**, 201-216.

Charney, J., W. J. Quirk, S.-H. Chow, and J. Kornfield, 1977: A comparative study of the effects of albedo change on drought in semi-arid regions. *J. Atmos. Sci.*, **34**, 1366-1385.

Chen, T.-C. and M.-C. Yen, 1993: The effect of planetary-scale divergent circulation on the interannual variation of the summertime stationary eddies: The tropical easterly jet. *Tellus*, **45A**, 15-27.

Chen, T.-C. and M.-C. Yen, 1994: Interannual variation of the Indian monsoon simulated by the NCAR Community Climate Model: Effect of the tropical Pacific SST. *J. Climate*, **7**, 1403-1415.

Clarke, A.J., X. Liu, and S. Van Gorder, 1996: On the dynamics of the biennial oscillation in the equatorial Indian and far western Pacific Oceans. *J. Climate*, submitted.

Clemens, S.C., and R.J. Oglesby, 1992: Interhemispheric moisture transport in the Indian Ocean summer monsoon: Data-model and model-model comparisons. *Paleoceanogr.*, **7**, 633-643.

Douville, H., and J.-F. Royer, 1996: Sensitivity of the Asian summer monsoon to an anomalous Eurasian snow cover within the Meteo-France GCM. *Cli. Dyn.*, **12**, 449-466.

Gray, W.M., J.D. Sheaffer, and J.A. Knaff, 1992: Influence of the stratospheric QBO on ENSO variability. *J. Meteorol. Soc. Japan*, **70**, 975-995.

Goswami, B.N., 1995: A multiscale interaction model for the origin of the tropospheric QBO. *J. Climate*, **8**, 524-534.

Goswami, B.N. and S. Manabe, 1996: A multiscale interaction model for the origin of the tropospheric QBO. *J. Climate*, submitted.

Groisman, P.Y., T.R. Karl, and R.W. Knight, 1994: Changes in snow cover, temperature, and radiative heat balance over the Northern Hemisphere. *J. Climate*, **7**, 1633-1656.

Hahn, D.J. and J. Shukla, 1976: An apparent relationship between Eurasian snow cover and Indian monsoon rainfall. *J. Atmos. Sci.*, **33**, 2461-2462.

Halpert, M.S. and C.F. Ropelewski, eds., 1991: Climate Assessment, A Decadal Review 1981-1990. U.S. Department of Commerce, Camp Springs, Md., 109 pp.

Halpert, M.S. and C.F. Ropelewski, 1992: Surface temperature patterns associated with the Southern Oscillation. *J. Climate*, **5**, 577-593.

Hastenrath, S., A. Nicklis, and L. Greischar, 1993: Atmospheric-hydrospheric mechanisms of climate anomalies in the western equatorial Indian Ocean. *J. Geophys. Res.*, **98**, 20219-20235.

Jiang, N., J.D. Neelin, and M. Ghil, 1995: Quasi-quadrennial and quasi-biennial variability in the equatorial Pacific. *Cli. Dyn.*, **12**, 101-112.

Jin, F.-F., J.D. Neelin, and M. Ghil, 1994: El Nino on the Devil's Staircase: Annual subharmonic steps to chaos. *Science*, **264**, 70-72.

Ju, J. and J. Slingo, 1995: The Asian summer monsoon and ENSO. *Q. J. Roy. Meteorol. Soc.*, **121**, 1133-1168.

Kiladis, G.N. and H. van Loon, 1988: The Southern Oscillation. Part VII: Meteorological anomalies over the Indian and Pacific sectors associated with the extremes of the oscillation. *Mon. Wea. Rev.*, **116**, 120-136.

Kiladis, G.N. and Diaz, H.F., 1989: Global climatic anomalies associated with extremes in the Southern Oscillation. *J. Climate*, **2**, 1069–1090.

Kitoh, A., 1992: Simulated interannual variations of the Indo-Australian monsoons. *J. Meteorol. Soc. Japan*, **70**, 563–583.

Krishnamurti, T.N., H.S. Bedi, and M. Subramanian, 1989: The summer monsoon of 1987. *J. Climate*, **4**, 321–340.

Krishnamurti, T.N., H.S. Bedi, and M. Subramanian, 1990: The summer monsoon of 1988. *Meteorol. Atmos. Phys.*, **42**, 19–37.

Kutzbach, J.E., W.L. Prell, and Wm. F. Ruddiman, 1993: Sensitivity of Eurasian climate to surface uplift of the Tibetan Plateau. *J. Geology*, **101**, 177-190.

Kutsuwada, K., 1991: Quasi-periodic variabilities of wind-stress fields over the Pacific Ocean related to ENSO events. *J. Meteorol. Soc. Japan*, **69**, 687–699.

Lamb, PJ and R.A. Peppler, 1991: West Africa. in *Teleconnections Linking Worldwide Climate Anomalies*, M. Glantz, R.W. Katz, and N. Nicholls, eds., Cambridge Univ. Press, Cambridge, UK, 121–189.

Latif, M., A. Sterl, M. Assenbaum, M.M. Junge, and E. Maier-Reimer, 1994: Climate variability in a coupled GCM. Part II: The Indian Ocean and monsoon. *J. Climate*, **7**, 1449–1462.

Lau, K.-M., 1992: East Asian summer monsoon rainfall variability and climate teleconnection. *J. Meteorol. Soc. Japan*, **70**, 211-242.

Lau, K.-M., and P.J. Sheu, 1988: Annual cycle, quasi-biennial oscillation, and Southern Oscillation in global precipitation. *J. Geophysical Res.*, **93**, 10,975-10,988.

Lau, K.-M. and S. Yang, 1996: The Asian monsoon and predictability of the tropical ocean-atmosphere system. *Q. J. Roy. Meteorol. Soc.*, in press.

Li, C., and M. Yanai, 1996: The onset and interannual variability of the Asian summer monsoon in relation to land-sea thermal contrast. *J. Climate*, **9**, 358–375.

Lofgren, B.M., 1995: Sensitivity of land-ocean circulations, precipitation, and soil moisture to perturbed land surface albedo. *J. Climate*, **8**, 2521–2542.

Lukas, R. 1988: Interannual fluctuations of the Mindanao Current inferred from sea level. *J. Geophys. Res.*, **93**, 6744–6748.

Marengo, J.A., and S. Hastenrath, 1993: Case studies of extreme climatic events in the Amazon Basin. *J. Climate*, **6**, 617–627.

Masumoto, Y., and T. Yamagata, 1991: The response of the western tropical Pacific to the Asian winter monsoon: The generation of the Mindanao Dome. *J. Phys. Oceanogr.*, **21**, 1386–1398.

Meehl, G.A., 1987: The annual cycle and interannual variability in the tropical Indian and Pacific Ocean regions. *Mon. Wea. Rev.*, **115**, 27 50.

Meehl, G.A., 1988: Tropical-midlatitude interactions in the Indian and Pacific sectors of the Southern Hemisphere. *Monthly Weather Review*, **116**, 472–484.

Meehl, G.A., 1989: The coupled ocean-atmosphere modeling problem in the tropical Pacific and Asian monsoon regions. *Journal of Climate*, **2**, 1146–1163.

Meehl, G.A., 1990: Seasonal cycle forcing of El Nino - Southern Oscillation in a global, coupled ocean-atmosphere GCM. *J. Climate*, **3**, 72-98.

Meehl, G.A., 1993: A coupled air-sea biennial mechanism in the tropical Indian

and Pacific regions: Role of the ocean. *J. Climate*, **6**, 31–41.

Meehl, G.A., 1994a: Coupled land–ocean–atmosphere processes and south Asian monsoon variability. *Science*, **266**, 263–267.

Meehl, G.A., 1994b: Influence of the land surface in the Asian summer monsoon: External conditions versus internal feedbacks. *J. Climate*, **7**, 1033–1049.

Meehl, G.A., G.W. Branstator, and W.M. Washington, 1993: Tropical Pacific interannual variability and CO_2 climate change. *J. Climate*, **6**, 42–63.

Meehl, G.A., and W.M. Washington, 1993: South Asian summer monsoon variability in a model with doubled atmospheric carbon dioxide concentration. *Science*, **260**, 1101–1104.

Meehl, G.A., M. Wheeler, and W.M. Washington, 1994: Low-frequency variability and CO2 transient climate change. Part 3. Intermonthly and interannual variability. *Clim. Dyn.*, **10**, 277–303.

Murakami, T. and B. Wang, 1993: Annual cycle of equatorial east-west circulation over the Indian and Pacific Oceans. *J. Climate*, **6**, 932–952.

Nicholls, N., 1978: Air-sea interaction and the quasi-biennial oscillation. *Mon. Wea. Rev.*, **106**, 1505–1508.

Nicholls, N., 1979: A simple air-sea interaction model. *Quart. J. Royal Meteorol. Soc.*, **105**, 93–105.

Nicholls, N., 1984: The Southern Oscillation and Indonesia sea surface temperature. *Mon. Wea. Rev.*, **112**, 424–432.

Nicholson, S.E., 1996: An analysis of the ENSO signal in the tropical Atlantic

and western Indian Oceans. *Int. J. Climatol.*, submitted.

Nigam, S., 1994: On the dynamical basis for the Asian summer monsoon rainfall-El Nino relationship. *J. Climate*, **7**, 1750–1771.

Palmer, T.N., C. Brankovic, P. Viterbo, and M.J. Miller, 1992: Modeling interannual variations of summer monsoons. *J. Climate*, **5**, 399–417.

Parthasarathy, B., K. Rupa Kumar, and A.A. Munot, 1991: Evidence of secular variations in Indian monsoon rainfall-circulation relationships. *J. Climate*, **4**, 927-938.

Rasmusson, E.M., and T.H. Carpenter, 1983: The relationship between eastern equatorial Pacific sea surface temperatures and rainfall over India and Sri Lanka. *Mon. Wea. Rev.*, **111**, 517-528.

Rasmusson, E.M., X. Wang, and C.F. Ropelewski, 1990: The biennial component of ENSO variability. *J. Mar. Sys.*, **1**, 71-90.

Ropelewski, C.F. and Halpert, M.S., 1987: Global and regional scale precipitation patterns associated with the El Nino/Southern Oscillation. *Mon. Wea. Rev.*, **115**, 1606–1626.

Ropelewski, C.F. and Halpert, M.S., 1989: Precipitation patterns associated with the high index phase of the Southern Oscillation. *J. Climate*, **2**, 268–284.

Ropelewski, C.F. M.S. Halpert, and X. Wang, 1992: Observed tropospheric biennial variability and its relationship to the Southern Oscillation. *J. Climate*, **5**, 594–614.

Sankar-Rao, M., K.M. Lau, and S. Yang, 1996: On the relationship between Eurasian snow cover and the Asian summer monsoon. *Int. J. Climatol.*, in press.

Shen, S., and K.-M. Lau, 1995: Biennial oscillation associated with the East Asian

summer monsoon and tropical sea surface temperature. *J. Meteorol. Soc. Japan*, **73**, 105–124.

Shukla, J., 1987: Interannual variability of monsoons. *Monsoons*, eds. J.S. Fein, P.L. Stephens, John Wiley and Sons, New York, 399-464.

Shukla, J. and Y. Mintz, 1982: Influence of land-surface evapotranspiration on the earth's climate. *Science*, **215**, 1498–1500.

Soman, J.K., and J. Slingo, 1996: Sensitivity of Asian summer monsoon to aspects of sea surface temperature anomalies in the tropical Pacific Ocean. *Q. J. Roy. Meteorol. Soc.*, submitted.

Terray, P., 1995: Space-time structure of monsoon interannual variability. *J. Climate*, **8**, 2595–2619.

Ting, M., 1994: Maintenance of northern summer stationary waves in a GCM. *J. Atmos. Sci.*, **51**, 3286–3308.

Tomita, T. and T. Yasunari, 1996: Role of the northeast winter monsoon on the biennial oscillation of the ENSO/monsoon system. *J. Meteorol. Soc. Japan*, submitted.

Trenberth, K.E., 1975: A quasi-biennial standing wave in the Southern Hemisphere and interrelations with sea surface temperature. *Quart. J. Royal Meteorol. Soc.*, **101**, 55-74.

Trenberth, K.E., 1992: Global analyses from ECMWF and atlas of 1000 to 10 mb circulation statistics. NCAR Technical Note NCAR/TN-373+STR, NCAR, Boulder CO, 191pp plus fiche.

van Loon, H., and J. Williams, 1977: The connection between trends of mean

temperature and circulation at the surface: Part IV. Comparison of the surface changes in the Northern Hemisphere with the upper air and with the Antarctic in winter. *Mon. Wea. Rev.*, **105**, 636–647.

Vernekar, A.D., J. Zhou and J. Shukla, 1994: The effect of Eurasian snow cover on the Indian monsoon. *J. Climate*, **8**, 248–266.

Ward, M.N., 1995: Analysing the Boreal Summer relationship between worldwide sea-surface temperature and atmospheric variability. In Analysis of Climate Variability, Eds H. von Storch and A. Navarra. Springer-Verlag. pp95-117.

Washington, W.M. and G.A. Meehl, 1989: Climate sensitivity due to increased CO_2: Experiments with a coupled atmosphere and ocean general circulation model. *Clim. Dyn.*, **4**, 1–38.

Webster, P.J., 1987: The elementary monsoon. *Monsoons*, Eds. J.S. Fein and P.L. Stephens, John Wiley and Sons, New York, 3-32.

Webster, P.J., and S. Yang, 1992: Monsoon and ENSO: Selectively interactive systems. *Q. J. Roy. Meteorol. Soc.*, **118**, 877-926.

Yang, S., 1996: ENSO-snow-monsoon associations and seasonal-interannual predictions. *Int. J. Climatol.*, in press.

Yang, S., K.-M. Lau, and M. Sankar-Rao, 1996: Precursory signals associated with the interannual variability of the Asian summer monsoon. *J. Climate*, in press.

Yang, S. and P.J. Webster, 1990: The effect of tropical heating in the adjacent hemisphere on the extratropical westerly jet streams. *J. Geophys. Res.*, **95**, 18705–18721.

Yasunari, T., 1990: Impact of Indian monsoon on the coupled atmosphere/ocean

system in the tropical Pacific. *Meteorol. Atmos. Phys.*, **44**, 29–41.

Yasunari, T., 1991: "The monsoon year"–a new concept of the climatic year in the tropics. *Bull. Am. Meteorol. Soc.*, **72**, 1331–1338.

Yasunari, T., A. Kitoh, and T. Tokioka, 1991: Local and remote responses to excessive snow mass over Eurasia appearing in the northern spring and summer climate—A study with the MRI-GCM. *J. Meteor. Soc. Japan*, **69**, 473-487.

Yasunari, T., and Y. Seki, 1992: Role of the Asian monsoon on the interannual variability of the global climate system. *J. Meteorol. Soc. Japan*, **70**, 177-189.

FIGURE CAPTIONS

Fig. 1: a) Schematic illustration of biennial atmosphere-ocean mechanism, b) same as (a) except for biennial atmosphere-land mechanism.

Fig. 2: General regions of anomalously wet (hatched) and dry (stippled) areas from station data for composites based on seasons the year before (year -1) and the year during (year 0) warm events in the Southern Oscillation, a) May-June-July year -1 (MJJ-1), b) November-December-January year -1 (NDJ-1), c) MJJ year 0, and d) NDJ year 0 (after Kiladis and van Loon, 1988).

Fig. 3: General regions of anomalously cold (stippled) and warm (hatched) areas from station data for composites based on seasons the year before (year -1), the year during (year 0), and the year after (year +1) warm events in the Southern Oscillation, a) May-June-July year -1 (MJJ-1), b) August-September-October year -1 (ASO-1), c) November-December-January year -1 (NDJ-1), d) February-March-April year 0 (FMA0), e) MJJ year 0, f) ASO year 0, g) NDJ year 0, h) FMA year +1 (after Kiladis and van Loon, 1988).

Fig. 4: a) Geographical pattern of EOF1 of global precipitation from stations using monthly precipitation anomalies (after Lau and Sheu, 1988), b) Power spectrum of the time series of the principal component of EOF1 shown in part (a), TBO and Southern Oscillation peaks as marked exceed the 95% confidence limit (after Lau and Sheu, 1988), c) same as (a) except for EOF2 from the coupled model, and d) same as (b) except for the EOF2 from the coupled model.

Fig. 5: a) Power spectrum of all-India monsoon index rainfall for the period 1901–1950, b) same as (a) except for a 50 year period from the coupled model. Ordinate units are mm^2 multiplied by a scaling factor. BW marked on figure is band width.

Fig. 6: a) Schematic of idealized biennial sequence of various monsoon-related quantities compiled from observed studies noted in text relative to strong monsoon season, noted JJA0, and the following year's weak monsoon, noted JJA+1, b) Actual biennial sequence for area-averaged quantities (areas noted in text) from the coupled model for strong minus weak composites relative to the strong monsoon season noted JJA0.

Fig. 7: a) Surface temperature anomalies representative of DJF0 (before a strong monsoon) for the coupled model formed from strong-minus-weak monsoon composites, positive contours are solid, and negative contours are dashed; b) same as (a) except for 500 mb height anomalies; c) same as (a) except for observed surface temperature differences, DJF 1988 minus 1987; d) same as (c) except for 500 mb height anomalies; e) same as (a) except for specified heating anomaly model described in text; f) same as (e) except for 500 mb height anomalies from the specified heating anomaly model. The anomalous convective heating centers are designated by +, and cooling by - in (e) and (f). Major warm surface temperature areas in (a), (c), and (e) are denoted by W. Key negative or anomalously low 500 mb height centers are labeled with an H.

Fig. 8: Same as Fig. 7 except for the DJF season after a strong monsoon (and before a weak monsoon).

Fig. 9: Specified heating anomaly model experiment described in text for analog to a) MAM0 season following the DJF0 season and preceding a strong monsoon in Fig. 7e, surface temperature differences for a specified heat source placed at 120E–equator; b) same as (a) except for 500 mb height anomalies; c) same as (a) except for MAM+1 season following the DJF+1 season in Fig. 8e, with a specified heating anomaly at 150W–equator; d) same as (c) except for 500 mb height anomalies.

Fig. 10: Surface wind anomalies from an experiment with the atmospheric GCM where SSTs are held at the climatological values but land albedos are raised. The result

is a weakened south Asian monsoon as documented by Meehl (1994b) and evidenced by the northeasterly wind anomalies in the Arabian Sea and Bay of Bengal, in addition to the westerly surface wind anomalies in the equatorial Pacific for the JJA season depicted here.

Fig. 11: Schematic of idealized TBO seasonal evolution. Year 0 refers to calendar year of strong monsoon, year +1 to calendar year of following year with a weak monsoon. Stippled area indicates year 1 of the TBO seasonal cycle going from late northern spring of year 0 to late northern spring of year +1. An idealized TBO seasonal cycle 2 would follow TBO seasonal cycle 1 and proceed from the late northern spring of year +1 to late northern spring the following year.

Table 1: Area averaged coupled model precipitation anomalies (mm day^{-1}) for east Africa (5N-5S, 15E- 35E), Australian monsoon (5S-20S, 130E-150E), and the tropical Pacific (0-15N, 150E-170E); and observed area-averaged OLR anomalies (W m^{-2}) for east Africa (0-10N, 25E-40E), Australian monsoon (0-20S, 120E-140E), and tropical Pacific (10S-10N, 140E-165E). Areas are chosen to coincide with respective seasonal maxima of model precipitation and observed OLR. Underlined values are consistent with sign of specified heating anomalies in experiments described in text. Note that negative OLR anomalies are interpreted as analogs for positive precipitation anomalies.

	EAST AFRICA	AUSTRALIAN MONSOON	TROPICAL PACIFIC
COUPLED MODEL DFJ_0 PRECIP	+0.35	+0.02	+0.24
COUPLED MODEL DFJ_{+1} PRECIP	−0.24	+0.36	−0.08
OLR DJF_0 (1988-87)	−3.46	+9.95	+1.38
OLR DJF_{+1} (1989-88)	+5.67	−6.67	+2.61

BIENNIAL ATMOSPHERE-OCEAN MECHANISM

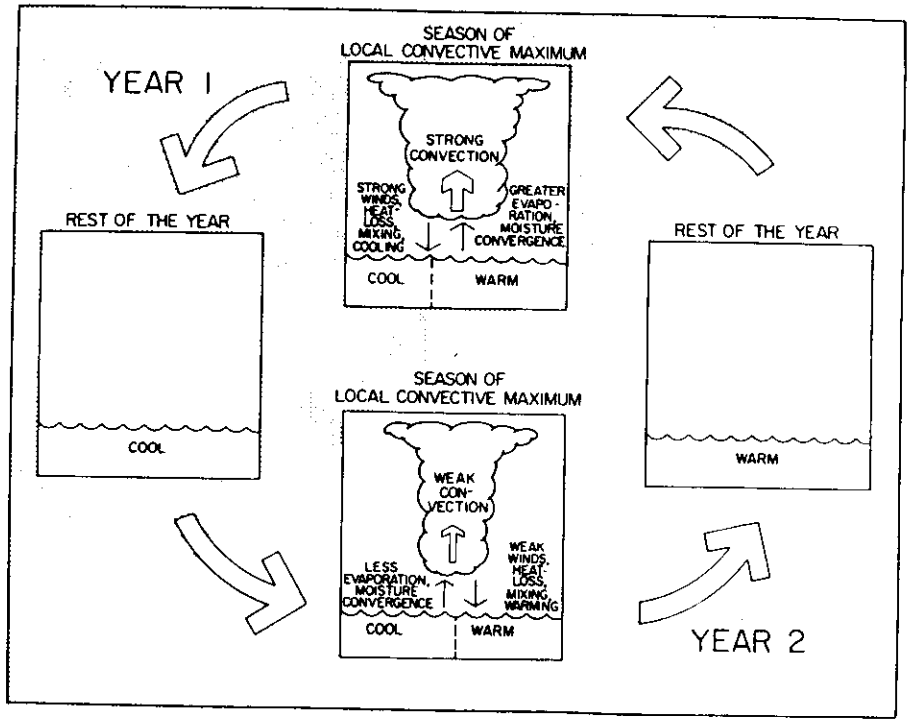

(1a)

BIENNIAL ATMOSPHERE-LAND MECHANISM

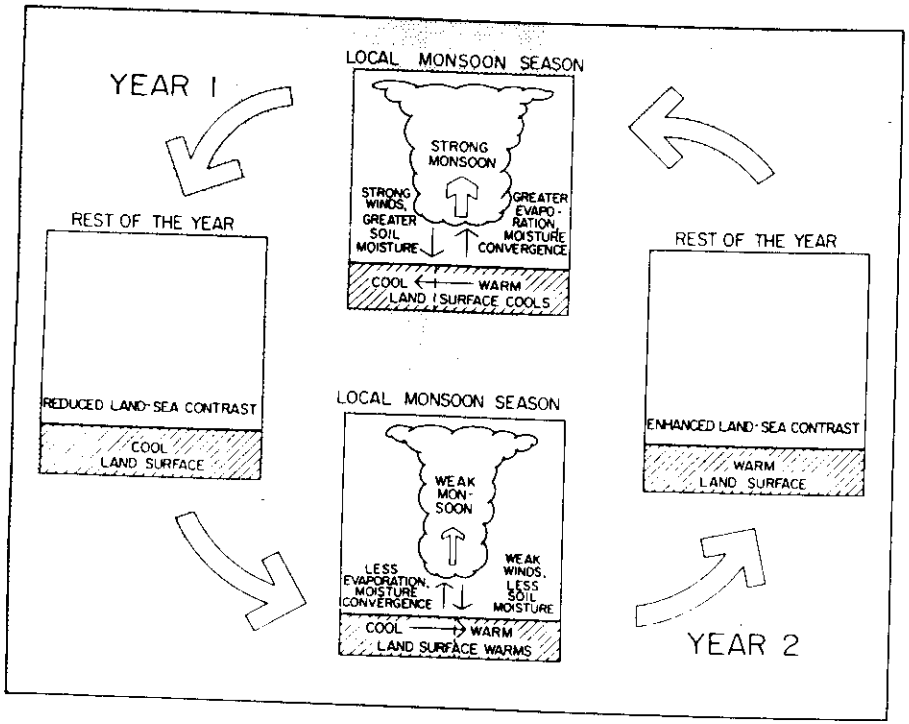

(1b)

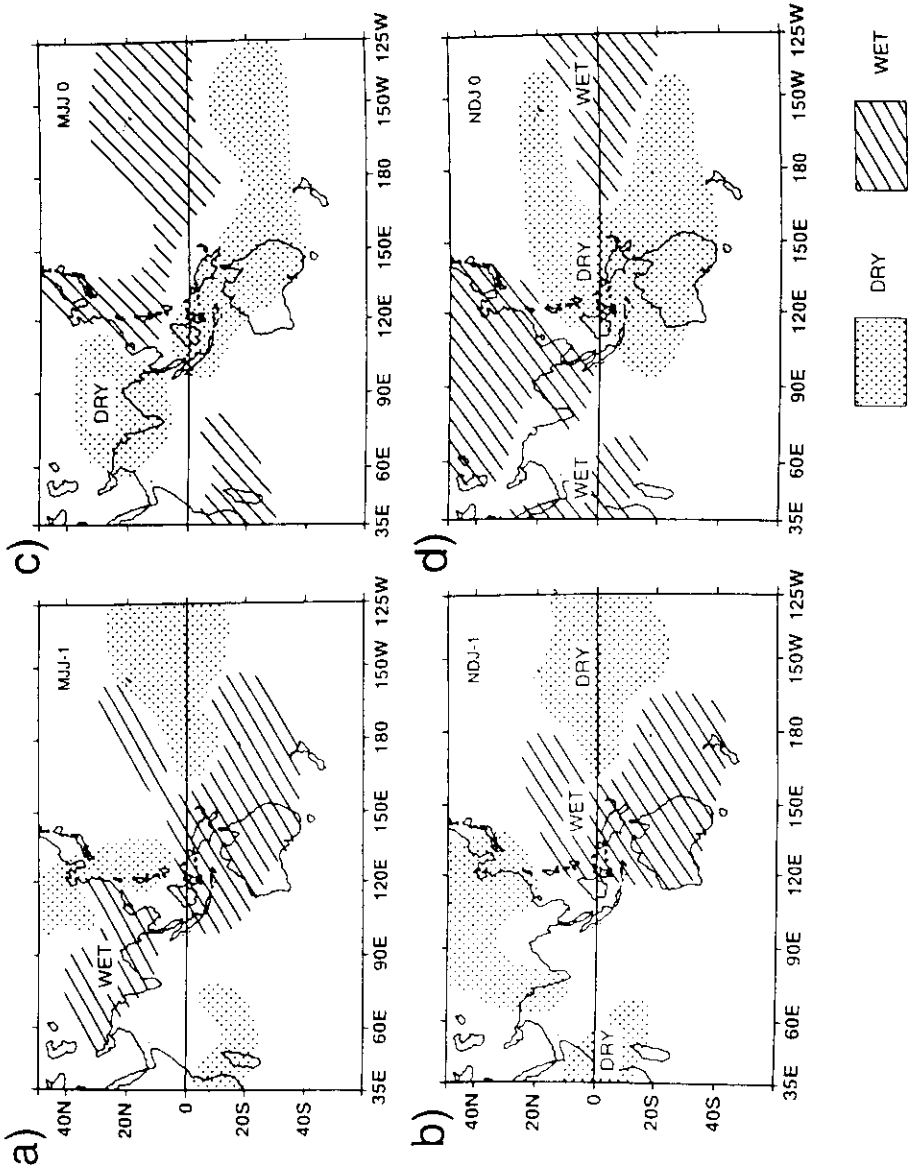

(2)

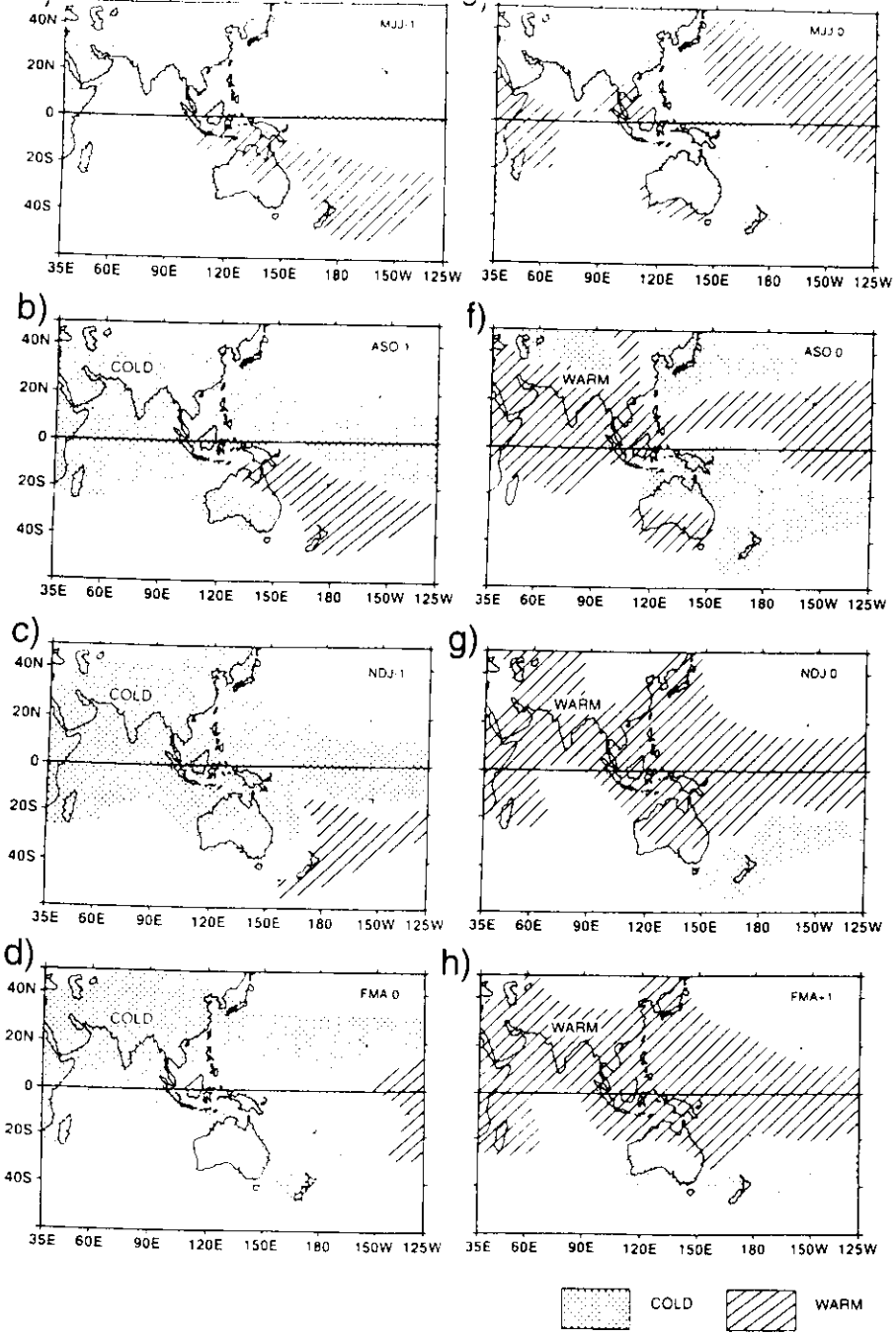

a)

EOF1, OBSERVED MONTHLY STATION PRECIPITATION

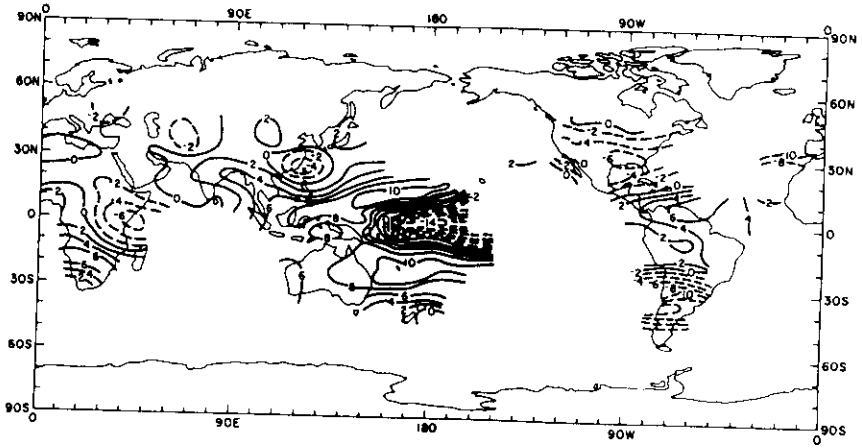

b)

POWER SPECTRUM OF OBSERVED MONTHLY GLOBAL PRECIPITATION

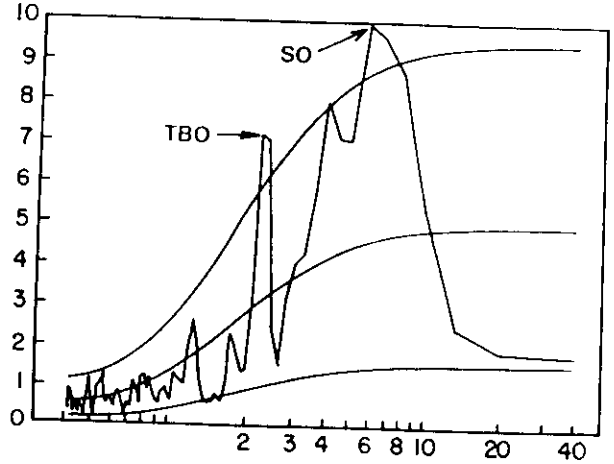

PERIOD (YEARS)

c)

EOF2, COUPLED MODEL MONTHLY PRECIPITATION

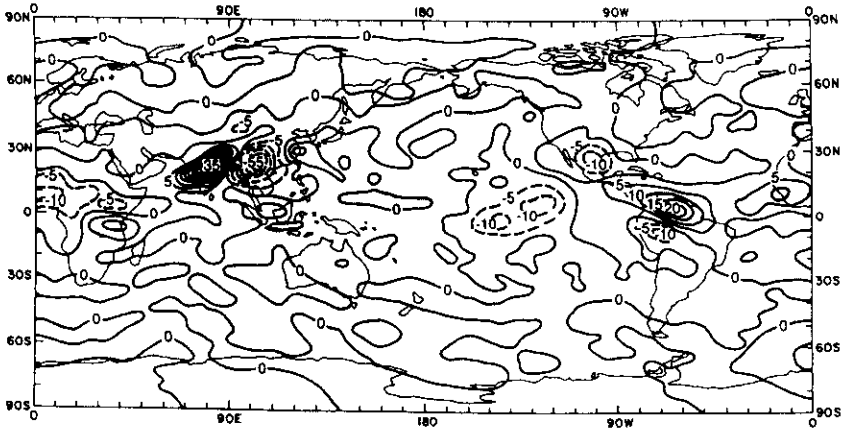

d)

CONTROL COUPLED PRECIP EOF2

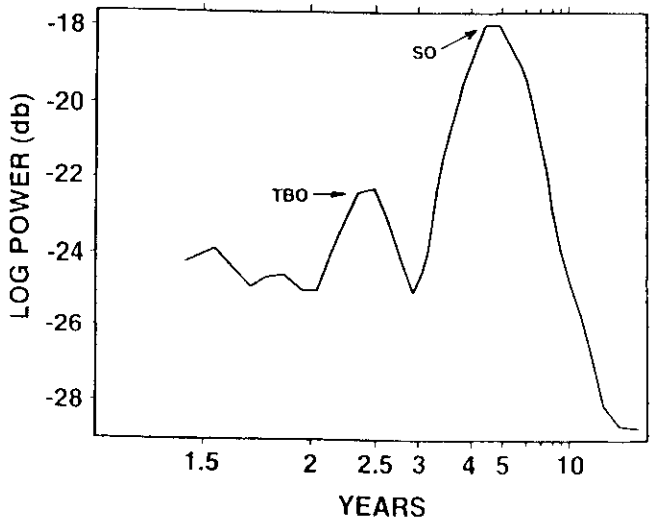

POWER SPECTRUM OF OBSERVED ALL- INDIA MONSOON PRECIPITATION INDEX, 1901-1950

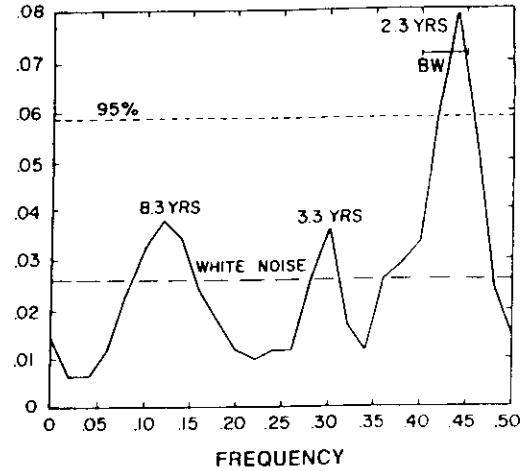

POWER SPECTRUM OF MONSOON SEASON RAINFALL, COUPLED MODEL

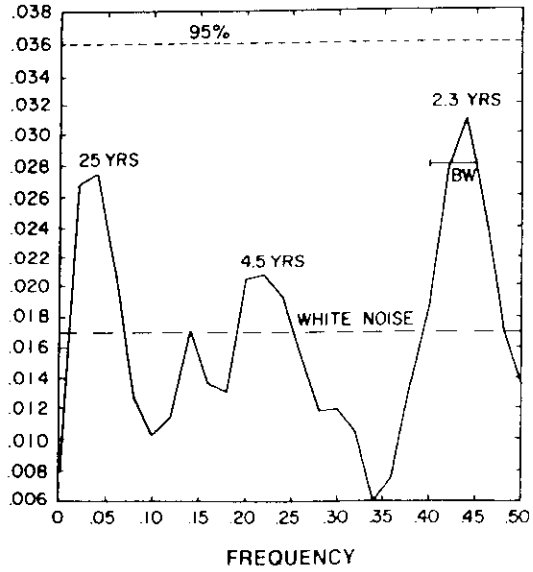

4 c d

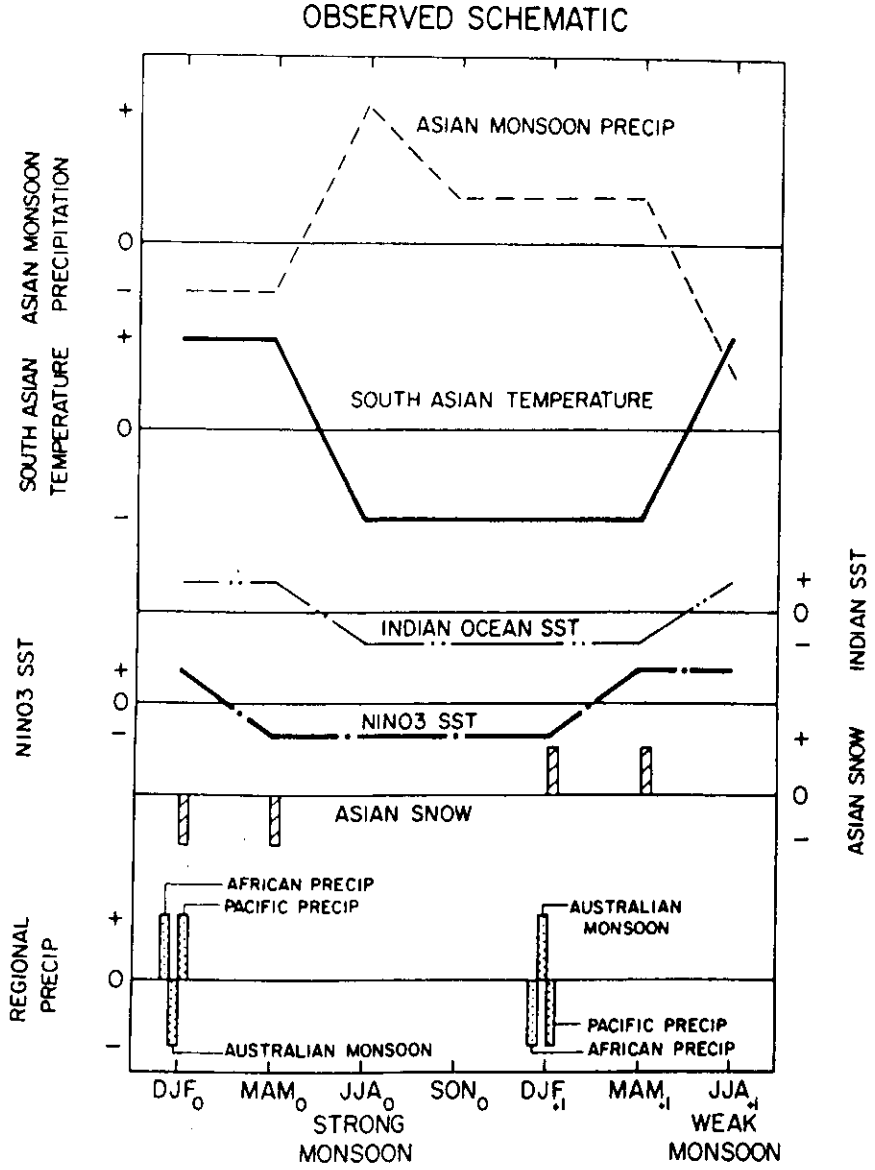
OBSERVED SCHEMATIC
ASIAN MONSOON PRECIP
SOUTH ASIAN TEMPERATURE
INDIAN OCEAN SST
NINO3 SST
ASIAN SNOW
AFRICAN PRECIP
PACIFIC PRECIP
AUSTRALIAN MONSOON
AUSTRALIAN MONSOON
PACIFIC PRECIP
AFRICAN PRECIP
SOUTH ASIAN TEMPERATURE
ASIAN MONSOON PRECIPITATION
NINO3 SST
INDIAN SST
ASIAN SNOW
REGIONAL PRECIP
DJF0 MAM0 JJA0 SON0 DJF+1 MAM+1 JJA+1
STRONG MONSOON
WEAK MONSOON

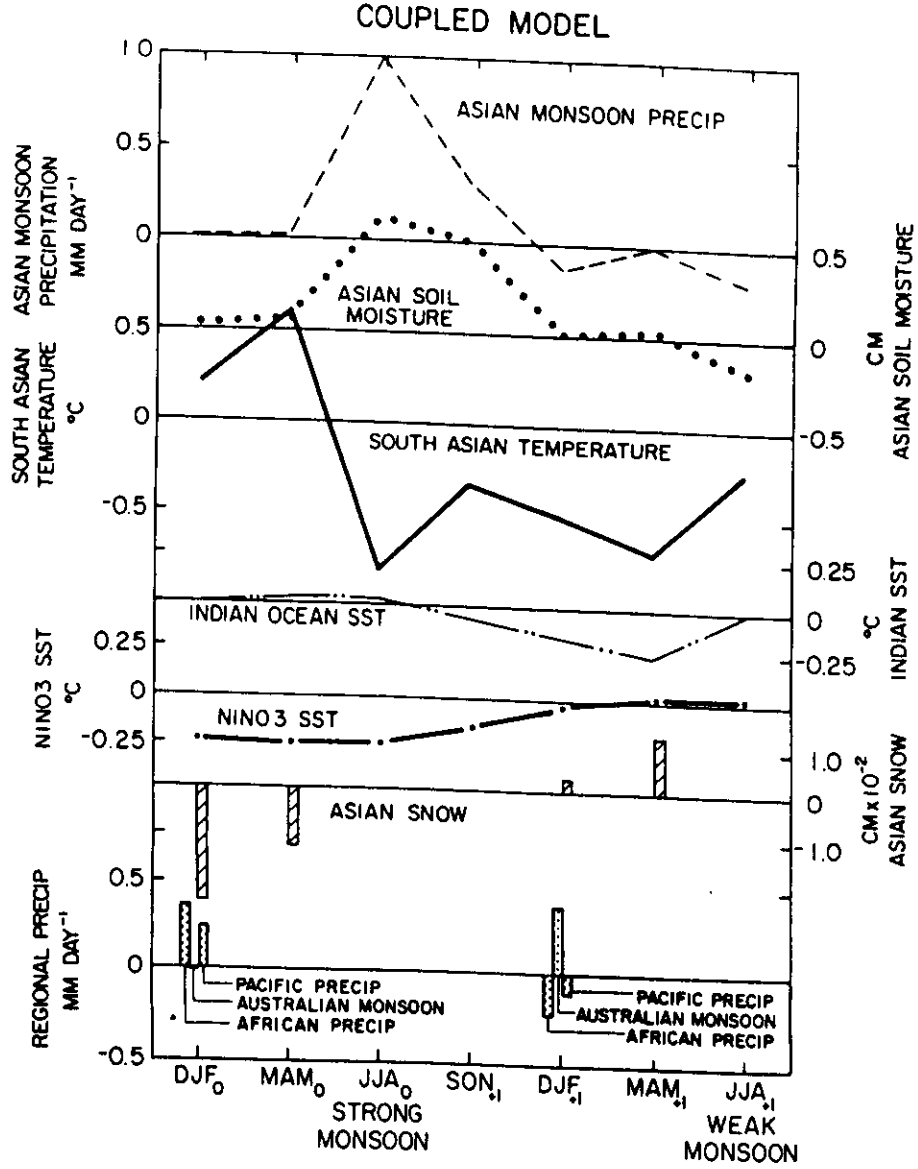
COUPLED MODEL
ASIAN MONSOON PRECIP
ASIAN SOIL MOISTURE
SOUTH ASIAN TEMPERATURE
INDIAN OCEAN SST
NINO3 SST
ASIAN SNOW
PACIFIC PRECIP
AUSTRALIAN MONSOON
AFRICAN PRECIP
PACIFIC PRECIP
AUSTRALIAN MONSOON
AFRICAN PRECIP
SOUTH ASIAN TEMPERATURE °C
ASIAN MONSOON PRECIPITATION MM DAY⁻¹
NINO3 SST °C
INDIAN SST °C
ASIAN SNOW CM x 10⁻²
REGIONAL PRECIP MM DAY⁻¹
CM ASIAN SOIL MOISTURE
DJF0 MAM0 JJA0 SON+1 DJF+1 MAM+1 JJA+1
STRONG MONSOON
WEAK MONSOON

A)

COUPLED MODEL DJF$_0$, SURFACE T DIFFERENCES

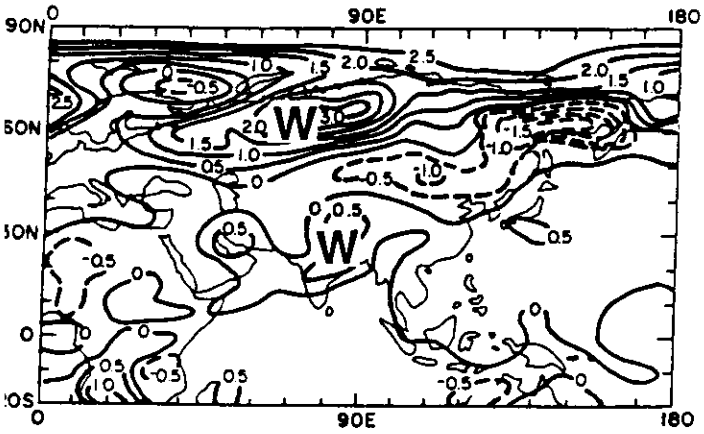

B)

COUPLED MODEL DJF$_0$, 500 MB Z DIFFERENCES

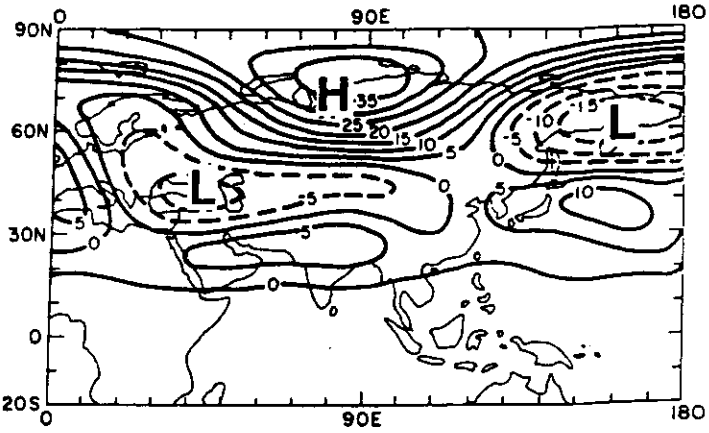

C)

ECMWF 1988 MINUS 1987, DJF, SURFACE T DIFFERENCES

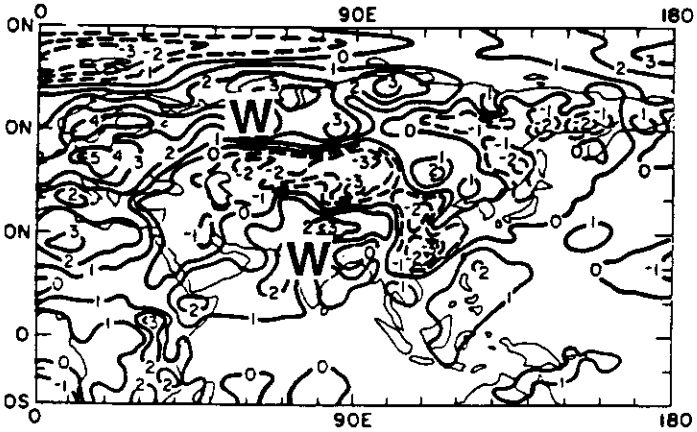

D)

ECMWF 1988 MINUS 1987, DJF, 500 MB Z DIFFERENCES

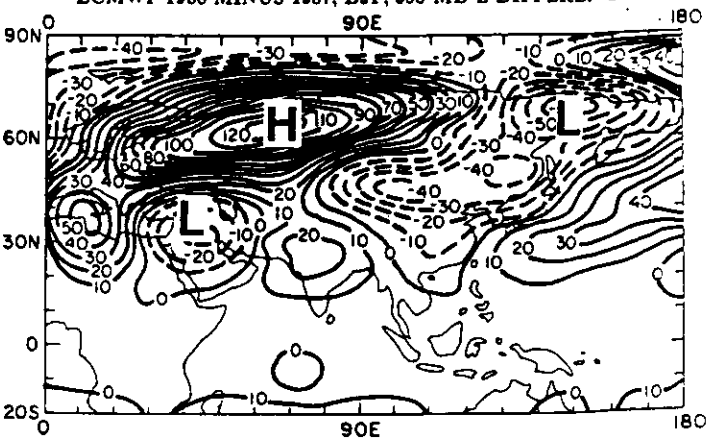

E)

SPECIFIED HEATING ANOMALIES DJF$_0$, SURFACE T DIFFERENCES

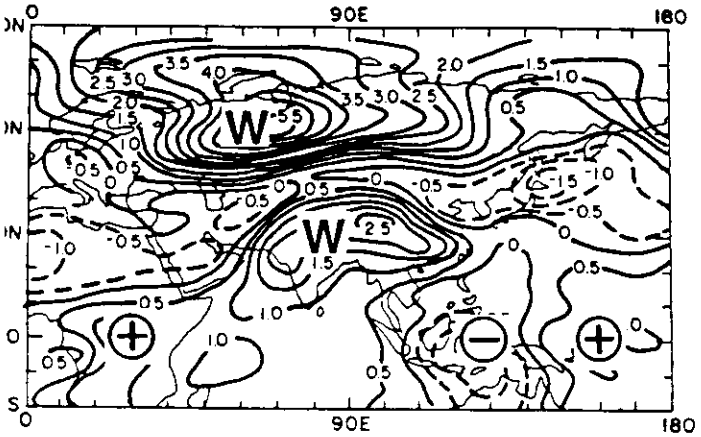

F)

SPECIFIED HEATING ANOMALIES DJF$_0$, 500 MB Z DIFFERENCES

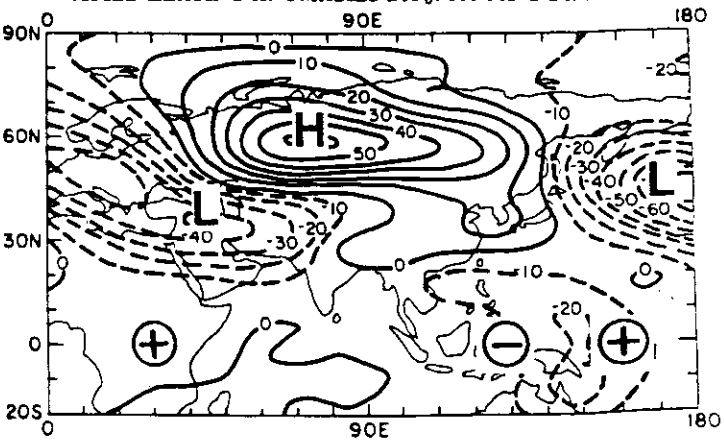

A)

COUPLED MODEL, DJF$_{+1}$, SURFACE T DIFFERENCES

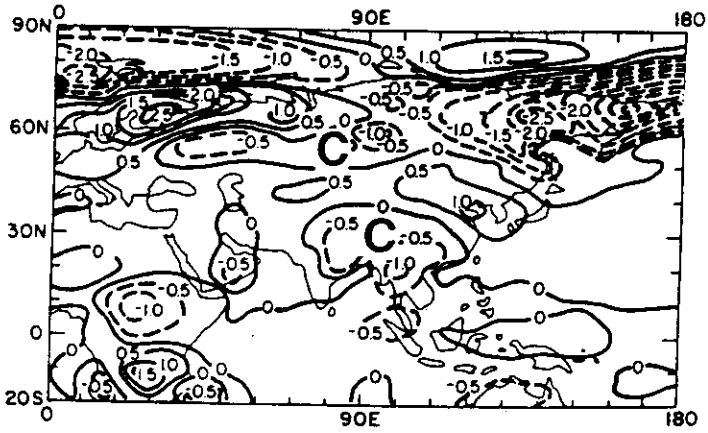

B)

COUPLED MODEL, DJF$_{+1}$, 500 MB Z DIFFERENCES

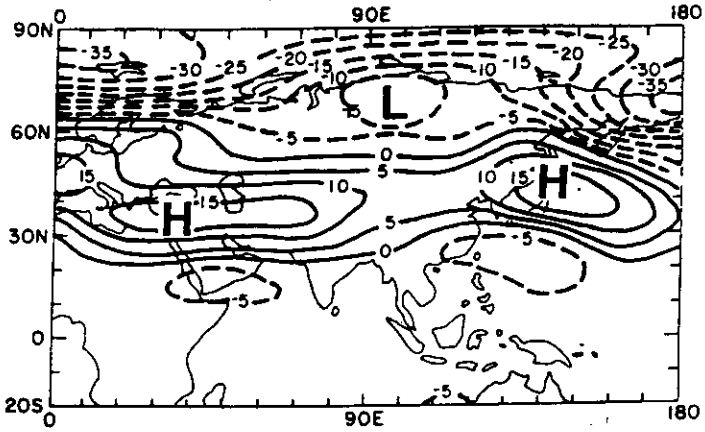

C)

ECMWF 1989 MINUS 1988, DJF, SURFACE T DIFFERENCES

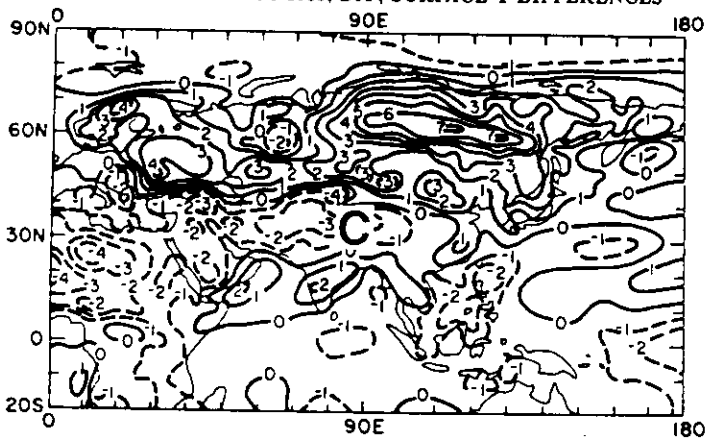

D)

ECMWF 1989 MINUS 1988, DJF, 500 MB Z DIFFERENCES

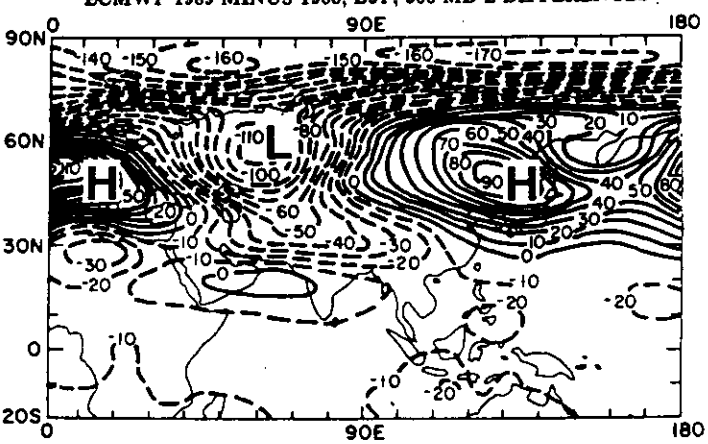

E)

SPECIFIED HEATING ANOMALIES DJF$_{+1}$, SURFACE T DIFFERENCES

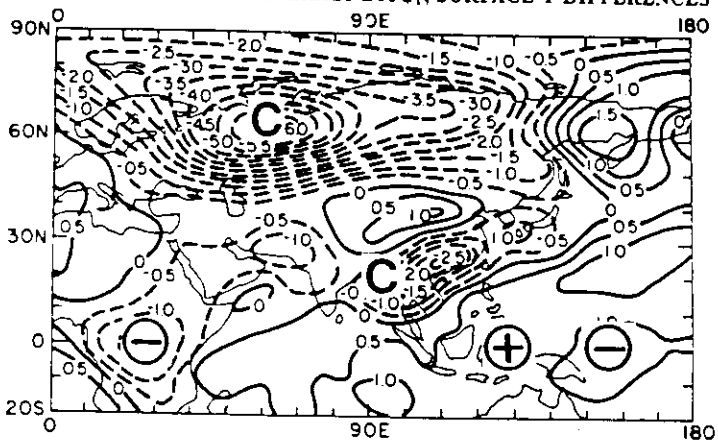

F)

SPECIFIED HEATING ANOMALIES DJF$_{+1}$, 500 MB Z DIFFERENCES

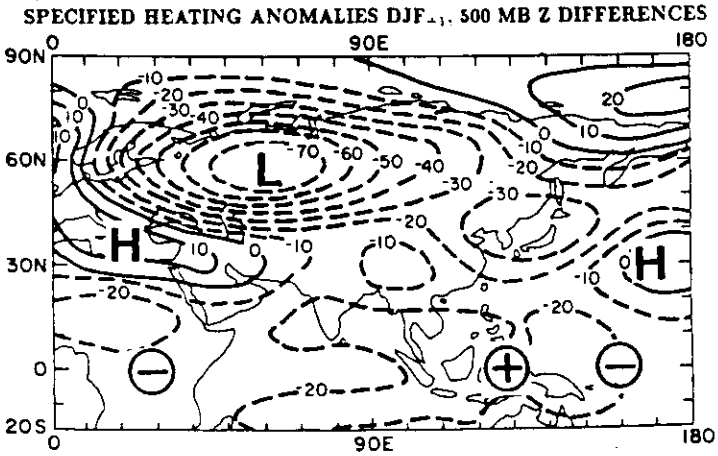

A) SPECIFIED HEATING ANOMALY (120E, EQ) MAM_0 ANALOG, SURFACE T DIFFERENCES

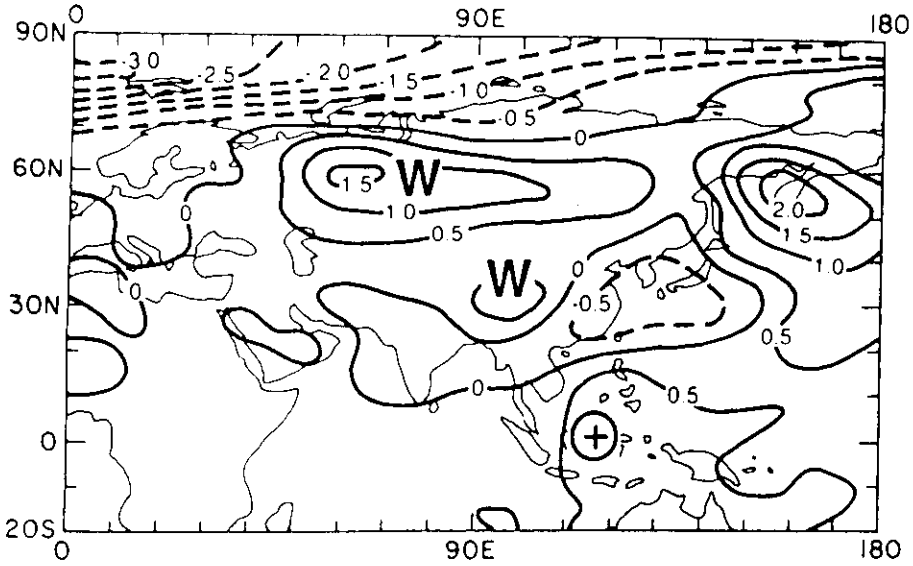

B) SPECIFIED HEATING ANOMALY (120E, EQ) MAM_0 ANALOG, 500MB Z DIFFERENCES

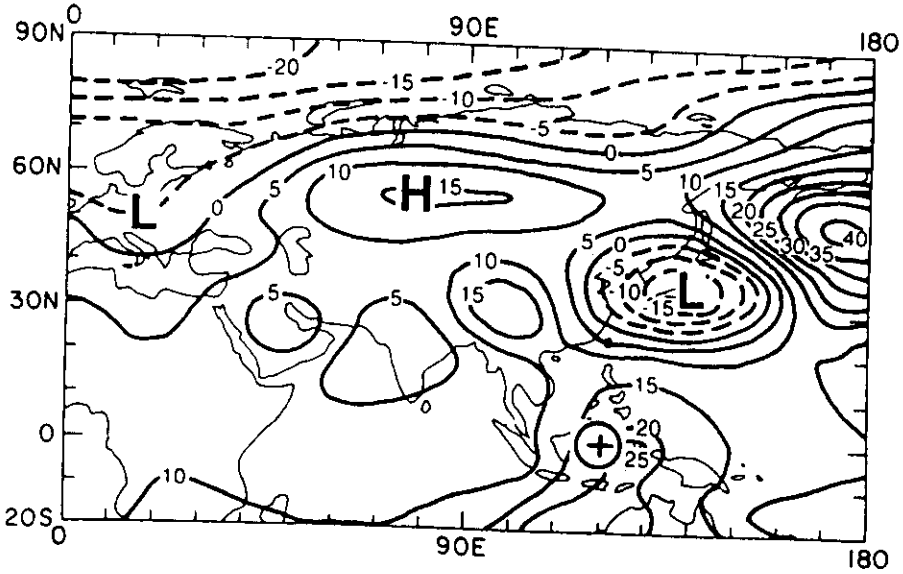

C) SPECIFIED HEATING ANOMALY (150W, EQ) MAM_{+1} ANALOG, SURFACE T DIFFERENCES

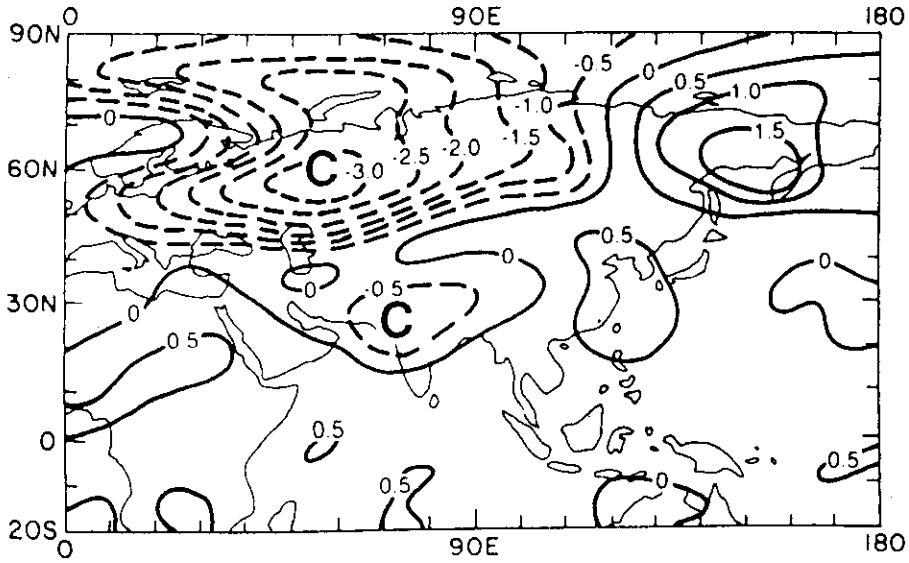

D) SPECIFIED HEATING ANOMALY (150W, EQ) MAM_{+1} ANALOG, 500MB Z DIFFERENCES

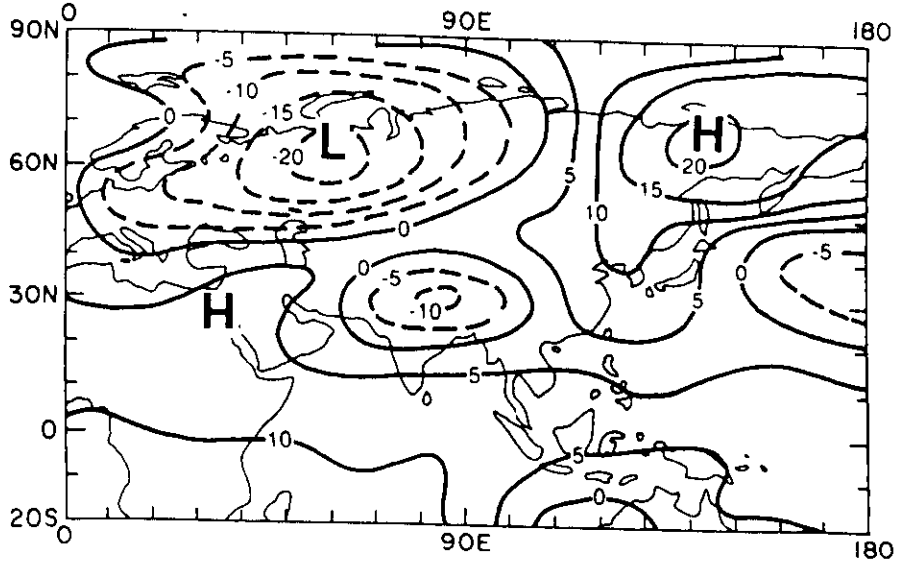

JJA Surface Wind Anomalies, Weak Monsoon Minus Control

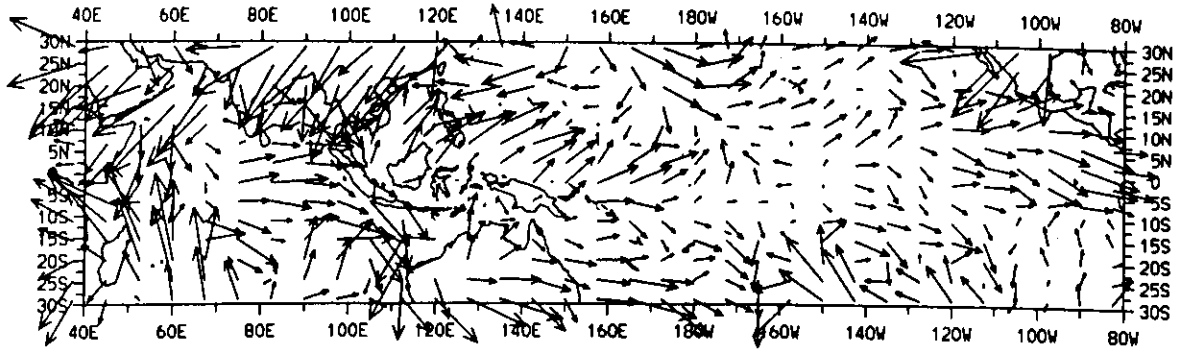

→ 1m sec $^{-1}$

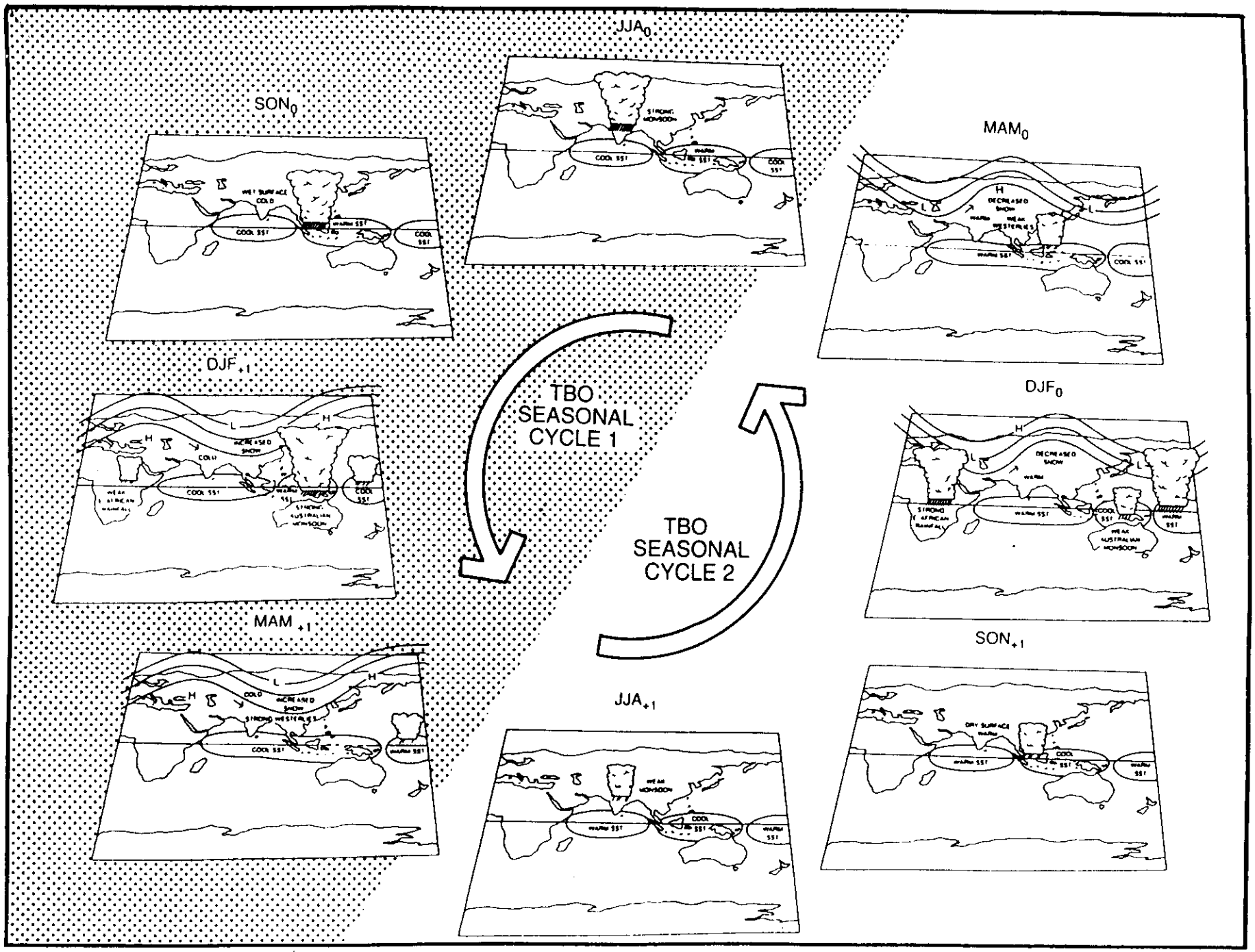
JJA0
SON0
MAM0
DJF+1
DJF0
TBO SEASONAL CYCLE 1
TBO SEASONAL CYCLE 2
MAM +1
SON+1
JJA+1